Supporting Information

for

Stability of half-sandwich Os(II) complex with indomethacin-functionalized ligand in the presence of carboxypeptidase A

Lukáš Masaryk,[a] Darina Muthná,[b] Petr Halaš,[a] Pavel Zoufalý,[a] Eva Peterová,[b] Radim Havelek,[b] Bohuslav Drahoš,[a] David Milde,[c] Alena Mrkvicová[b] and Pavel Štarha*[a]

[a] Department of Inorganic Chemistry, Faculty of Science, Palacký University in Olomouc, 17. listopadu 12, 771 46 Olomouc, Czech Republic

[b] Department of Medical Biochemistry, Faculty of Medicine in Hradec Kralove, Charles University in Prague, Šimkova 870, 500 03 Hradec Kralove, Czech Republic

[c] Department of Analytical Chemistry, Faculty of Science, Palacký University in Olomouc, 17. listopadu 12, 771 46 Olomouc, Czech Republic

Correspondence:

Assoc. Prof. Pavel Štarha, Ph.D.

E-mail: pavel.starha@upol.cz

Table of Contents

Experimental Section

Materials

Chemicals ($OsCl_3 \cdot nH_2O$, α-terpinene, ammonium hexafluorophosphate (NH_4PF_6), 2-pyridinecarbonitrile, thiosemicarbazide, trifluoroacetic acid (TFA), indomethacin, carbonyldiimidazole (CDI), ammonia (25% solution in water), phosphate-buffered saline (PBS), silver nitrate ($AgNO_3$), carboxypeptidase A from bovine pancreas, potassium chloride (KCl), Lawesson's reagent, triethylamine, oxalyl chloride), formic acid, solvents (methanol (MeOH), diethyl ether (Et_2O), ethanol, chloroform, *N,N*-dimethylformamide (DMF), dimethyl sulfoxide (DMSO), acetone, *n*-octanol), deuterated solvents for NMR experiments (DMSO-d_6, D_2O) and HPLC (H_2O and acetonitrile (MeCN)) were supplied by VWR International (Stříbrná Skalice, Czech Republic), Sigma-Aldrich (Prague, Czech Republic), Lach-Ner (Neratovice, Czech Republic) and Litolab (Chudobín, Czech Republic). The used chemicals and solvents were used as received, except DMF which was dried with molecular sieve pellets 4 Å. Macherey-Nagel TLC sheets ALUGRAM SILG/UV_{254} (silica gel 60) and silica gel 60 (0.015-0.040 mm) were employed for monitoring of reactions.

The starting dimeric Os(II) complex $[Os(\mu\text{-}Cl)(\eta^6\text{-}pcym)Cl]_2$ was synthesized in a Monowave 300 microwave reaction system (Anton Paar GmbH, Graz, Austria), as described previously.[1]

Synthesis of 5-(pyridin-2-yl)-1,3,4-thiadiazol-2-amine (L1)

Compound L1 was prepared according to a previously published procedure.[2] Briefly, 2-pyridinecarbonitrile (10 mmol) was mixed with thiosemicarbazide (11 mmol) in 20 mL of TFA. This solution was refluxed for 6 h. After that it was poured into 50 mL of distilled water and pH was then adjusted by aq. ammonia to 8. The resulting yellow precipitate was filtered off, washed with water and dried in a desiccator under reduced pressure. Yellow solid. Yield: 56%. $C_7H_6N_4S$ (MW = 178.21). Anal. Calc.: C, 47.2, H, 3.4, N, 31.4; found: C, 47.3, H, 3.6, N, 31.1%. ^{1}H NMR (400 MHz, DMSO-d_6, 298 K, ppm): 8.54 (d, J = 4.9 Hz, 1H, C9–H), 8.01 (d, J = 8.0 Hz, 1H, C12–H), 7.87 (t, J = 7.7 Hz, 1H, C11–H), 7.49 (s, 2H, N6–H), 7.38 (m, 1H, C10–H). ^{13}C NMR (400 MHz, DMSO-d_6, 298 K, ppm): 170.1 (C5), 158.4 (C7), 149.6 (C9–H), 137.4 (C11–H), 124.3 (C10–H), 119.0 (C12–H). IR (ATR, υ, cm^{-1}): 3249,

3040, 2949, 2759, 2687, 1639, 1617, 1583, 1561, 1506, 1489, 1447, 1431, 1334, 1304, 1274, 1247, 1126, 1066, 1008, 779, 740, 713, 619, 575, 507, 451, 403.

Synthesis of 1-(4-chlorobenzoyl)-5-methoxy-2-methyl-1H-indol-3-yl)-N-(5-(pyridin-2-yl)-1,3,4-thiadiazol-2-yl)acetamide (L2)

In a vial, indomethacin (0.70 mmol) was dissolved in 5 mL of dry DMF and CDI (0.70 mmol) was added. To reduce the absorption of air moisture, vial was capped with a needle pierced cap in order to allow evolved CO_2 gas to escape. This was then stirred at 100° C for 30 min. Then, 5-(pyridin-2-yl)-1,3,4-thiadiazol-2-amine (0.63 mmol, 0.9 molar equiv.) was added, and the reaction mixture was again capped and stirred at 120 °C for 18 h. This solution was then poured into 25 mL of distilled water and pH was adjusted to 8–9 by aq. ammonia. Resulting precipitate was then filtered off, washed thoroughly with water and dried in a desiccator under reduced pressure. White solid. Yield: 75%. $C_{26}H_{20}N_5ClO_3S$ (MW = 517.98). Anal. Calc.: C, 60.3, H, 3.9, N, 13.5; found: C, 60.4, H, 3.6, N, 13.2%. ^{1}H NMR (400 MHz, DMSO-*d*$_6$, 298 K, ppm): 12.94 (s, 1H, N6–H), 8.63 (d, *J* = 4.9 Hz, 1H, C9–H), 8.17 (d, *J* = 7.9 Hz, 1H, C12–H), 7.95 (t, *J* = 8.4 Hz, 1H, C11–H), 7.69–7.59 (m, 4H, C28,C29–H), 7.48 (t, *J* = 7.9 Hz, 1H, C10–H), 7.15 (s, 1H, C23–H), 6.94 (d, *J* = 9.0 Hz, 1H, C21–H), 6.69 (d, *J* = 9.0 Hz, 1H, C20–H), 3.96 (s, 2H, C15–H), 3.74–3.70 (m, 3H, C31–H), 2.27 (s, 3H, C25–H). ^{13}C NMR (400 MHz, DMSO-*d*$_6$, 298 K, ppm): 169.2 (C5), 167.9 (C14), 163.8 (C26), 160.1 (C16), 155.6 (C7), 150.0 (C9–H), 149.0 (C24), 137.8 (C11–H), 135.9 (C30), 134.1 (C17), 131.2–130.6 (C28,29–H), 130.2 (C27), 129.1 (C19), 125.4 (C10–H), 119.9 (C12–H), 114.7 (C21–H), 112.6 (C22), 111.3 (C20–H), 101.8 (C23–H), 55.5 (C31–H), 30.6 (C15–H), 13.4 (C25–H). IR (ATR, υ, cm^{-1}): 3144, 3000, 2927, 2831, 2719, 1670, 1588, 1556, 1478, 1433, 1398, 1358, 1325, 1290, 1232, 1174, 1152, 1087, 1069, 1035, 1013, 992, 959, 907, 828, 810, 786, 754, 716, 691, 659, 605, 592, 563, 534, 483, 438, 401.

Synthesis of (4-chlorophenyl){5-methoxy-2-methyl-3-[(5-(pyridin-2-yl)-1,3,4-thiadiazol-2-yl)methyl]-1H-indol-1-yl}methanone (L3)

The synthesis of intermediate **II** and ligand L3 was based on previously described procedures.[3] Briefly, to indomethacin (1.40 mmol) in 10 mL of $CHCl_3$ containing one drop of DMF, oxalyl chloride was added dropwise (7.88 mmol). The solution was stirred overnight under nitrogen without heating and afterwards dried under nitrogen. Subsequently, 20 mL of $CHCl_3$ was poured in

to dried chloride and solid picolinic acid hydrazide (1.40 mmol) was added along with triethylamine (2.10 mmol) in 2 mL $CHCl_3$. The solution was heated to reflux for 6 h, then evaporated and obtained solid washed repeatedly with water and methanol to obtain pure intermediate **II**. Compound **II** (1.05 mmol) and the Lawesson's reagent (1.57 mmol) in 30 mL of $CHCl_3$ were heated to 50 °C under nitrogen overnight. The solution was then evaporated and neutralized with $KHCO_3$ to pH 7–8. Filtrated solution offered yellowish solid, which was purified by a column chromatography (gradient: $CHCl_3$ (stab./amylene) to $CHCl_3$:CH_3OH = 40:1, *v/v*) and yielded white powder (L3) after the recrystallization in methanol.

For **II**: White solid. Yield: 83%. $C_{25}H_{21}ClN_4O_4$ (MW = 476.91). ^{1}H NMR (400 MHz, DMSO-d_6, 298 K, ppm): δ 10.51 (s, 1H), 10.30 (s, 1H), 8.66 (d, *J* = 4.6 Hz, 1H), 8.04–7.99 (m, 2H), 7.71–7.60 (m, 5H), 7.24 (d, *J* = 2.5 Hz, 1H), 6.94 (d, *J* = 8.9 Hz, 1H), 6.71 (d, *J* = 9.0 Hz, 1H), 3.81 (s, 3H), 3.65 (s, 2H), 2.28 (s, 3H). ^{13}C NMR (101 MHz, DMSO-d_6, 298 K, ppm): δ 168.4, 167.9, 162.8, 155.6, 149.1, 148.6, 137.8, 137.6, 135.3, 134.2, 131.2, 130.8, 130.2; 129.0, 127.0, 122.3, 114.4, 113.7, 111.5, 102.0, 55.4, 29.2, 13.4. ^{1}H NMR (400 MHz, $CDCl_3$, 298 K, ppm): δ 10.05 (d, *J* = 5.0 Hz, 1H), 8.56 (d, *J* = 4.8 Hz, 1H), 8.28 (d, *J* = 4.7 Hz, 1H), 8.09 (d, *J* = 7.8 Hz, 1H), 7.84 (d, *J* = 8.6 Hz, 1H), 7.71–7.66 (m, 2H), 7.51–7.44 (m, 3H), 7.01 (t, *J* = 2.7 Hz, 1H), 6.93–6.90 (m, 1H), 6.71 (d, *J* = 8.8 Hz, 1H), 3.84 (s, 3H), 3.80 (s, 2H), 2.43 (s, 3H). ^{13}C NMR (101 MHz, $CDCl_3$, 298 K, ppm): 168.4, 167.1, 161.1, 156.5, 148.7, 148.1, 139.6, 137.5, 136.7, 133.7, 131.4, 131.0, 130.2, 129.4, 127.1, 122.6, 115.3, 112.7, 111.6, 100.9, 55.9, 30.7, 13.6.

For L3: White solid. Yield: 57%. $C_{25}H_{19}ClN_4O_2S$ (MW = 474.96). Anal. Calc.: C, 63.2; H, 4.0; N, 11.8; found: C, 63.0; H, 4.1; N, 11.3. ^{1}H NMR (400 MHz, DMSO-d_6, 298 K, ppm): δ 8.60 (d, *J* = 4.9 Hz, 1H, C9–H), 8.18 (d, *J* = 7.9 Hz, 1H, C12–H), 7.98 (t, *J* = 7.7 Hz, 1H, C11–H), 7.62 (m, 4H, C28,29–H), 7.52 (m, 1H, C10–H), 7.15 (s, 1H, C23–H), 6.89 (d, *J* = 8.6 Hz, 1H, C21–H), 6.71 (d, *J* = 8.6 Hz, 1H, C20–H), 4.59 (s, 2H, C15–H), 3.72 (s, 3H, C31–H), 2.32 (s, 3H, C25–H). ^{1}H NMR (400 MHz, $CDCl_3$, 298 K, ppm): δ 8.56 (d, *J* = 4.5 Hz, 1H, C9–H), 8.30 (d, *J* = 7.9 Hz, 1H, C12–H), 7.82 (t, *J* = 7.7 Hz, 1H, C11–H), 7.66 (d, *J* = 8.4 Hz, 2H, C28–H), 7.46 (d, *J* = 8.4 Hz, 2H, C29–H), 7.34 (t, *J* = 6.6 Hz, 1H, C10–H), 6.96 (s, 1H, C23–H), 6.83 (d, *J* = 9.0 Hz, 1H, C21–H), 6.67 (d, *J* = 9.0 Hz, 1H, 20–H), 4.51 (s, 2H, C15–H), 3.79 (s, 3H, C31–H), 2.49 (s, 3H, C25–H). ^{13}C NMR (101 MHz, DMSO-d_6, 298 K, ppm): δ 171.2 (C5), 170.2 (C16), 167.9 (C26), 155.7 (C7), 150.1 (C9–H), 148.2 (C24), 137.9 (C11–H), 137.8 (C30), 135.4 (C17), 134.0 (C27), 131.3–129.1 (C19,28,29–H), 125.9 (C10–H), 120.2 (C12–H), 115.4 (C21–H), 114.8

(C22), 111.6 (C20–H), 101.6 (C23–H), 55.4 (C31–H), 24.4 (C15–H), 13.2 (C25–H). ^{13}C NMR (101 MHz, $CDCl_3$, 298 K, ppm): δ 171.7 (C5), 171.0 (C7), 168.4 (C26), 156.3 (C16), 149.8 (C9–H), 149.2 (C24), 139.6 (C30), 137.3 (C11–H), 135.8 (C17), 133.8 (C27), 131.3 (C19), 131.0–129.3 (C28,29–H), 125.4 (C10–H), 120.9 (C12–H), 115.6 (C21–H), 115.2 (C22), 112.2 (C20–H), 101.0 (C23–H), 55.9 (C31–H), 25.5 (C15–H), 13.4 (C25–H). IR (ATR, υ, cm^{-1}): 3321, 3092, 3064, 3037, 2991, 2964, 2928, 2825, 1669, 1606, 1586, 1568, 1476, 1452, 1434, 1399, 1371, 1310, 1263, 1244, 1225, 1176, 1151, 1125, 1090, 1061, 1038, 1008, 927, 895, 847, 806, 780, 754, 741, 714, 691, 664, 640, 616, 591, 553, 481, 435.

Synthesis of complexes 1–3

Complexes **1**–**3** were prepared by the reaction of $[Os(\mu\text{-}Cl)(\eta^6\text{-}pcym)Cl]_2$ (0.05 mmol) with L1–L3 (0.10 mmol), which were stirred in MeOH (5 mL) at ambient temperature for 24 h, leading to a change from an brown suspension to red solution of $[Os(\eta^6\text{-}pcym)(L)Cl]Cl$. Then, an excess of NH_4PF_6 (0.50 mmol) was added and after 5 min of stirring at ambient temperature, the reaction mixture was filtered and the solvent volume was reduced until the orange product precipitated. Complexes **1**–**3** were collected by filtration, washed (1 × 0.5 mL of MeOH and 3 × 1.0 mL of Et_2O) and dried in a desiccator under reduced pressure.

$[Os(\eta^6\text{-}pcym)(L1)Cl]PF_6$ (**1**): Red solid. Yield: 36%. $C_{17}H_{20}N_4ClF_6OsPS$ (MW = 683.08). Anal. Calc.: C, 29.9, H, 2.9, N, 8.2; found: C, 29.7, H, 2.8, N, 7.9%. ^{1}H NMR (400 MHz, DMSO, 298 K, ppm): δ 9.43 (d, *J* = 5.8 Hz, 1H, C9–H), 8.31 (m, 1H, C11–H), 8.21 (d, *J* = 7.9 Hz, 1H, C12–H), 7.76 (t, *J* = 7.9 Hz, 1H, C10–H), 6.50 (d, *J* = 5.9 Hz, 1H, C34–H), 6.44 (d, *J* = 5.9 Hz, 1H, C34–H), 6.19 (d, *J* = 5.8 Hz, 1H, C33–H), 6.08 (d, *J* = 5.9 Hz, 1H, C33–H), 2.66 (m, 1H, C37–H), 2.39 (s, 3H, C36–H), 1.12 (m, 6H, C38–H). ^{1}H NMR (400 MHz, D_2O-*d*$_6$, 298 K, ppm): δ 9.18 (d, *J* = 5.5 Hz, 1H, C9–H), 8.02 (t, *J* = 7.6 Hz, 1H, C11–H), 7.95 (d, *J* = 7.6 Hz, 1H, C12–H), 7.50 (t, *J* = 6.5 Hz, 1H, C10–H), 6.24 (d, *J* = 5.5 Hz, 1H, C33–H), 6.18 (d, *J* = 5.5 Hz, 1H, C33–H), 5.93 (d, *J* = 5.5 Hz, 1H, C34–H), 5.82 (d, *J* = 5.5 Hz, 1H, C34–H), 2.41 (m, *J* = 6.8 Hz, 1H, C37–H), 2.13 (s, 3H, C36–H), 0.87 (m, 6H, C38–H). ^{13}C NMR (101 MHz, DMSO, 298 K, ppm): δ 157.9 (C5), 155.6 (C9–H), 149.8 (C7), 140.7 (C11–H), 127.8 (C10–H), 124.8 (C12–H), 97.0 (C32), 95.8 (C35), 78.7–78.2 (C34–H), 75.0–73.9 (C33–H), 31.0 (C37–H), 22.0 (C38–H), 18.4 (C36–H). ESI+ MS (MeOH, *m/z*): 503.1 (calc. 503.1; 26%; $\{[Os(pcym)(L1)]–H\}^+$), 539.0 (calc. 539.1;

100%; [Os(pcym)(L1)Cl]$^+$). IR (ATR, ν, cm^{-1}): 375, 555, 741, 773, 826, 1035, 1035, 1163, 1315, 1413, 1474, 1513, 1606, 2869, 2965, 3058, 3120, 3362, 3443, 3626.

[Os(η^6-pcym)(L2)Cl]PF_6 (**2**): Red solid. Yield: 79%. $C_{36}H_{34}N_5Cl_2F_6O_3OsPS$ (MW = 1022.85). Anal. Calc.: C, 42.3, H, 3.4, N, 6.8; found: C, 42.7, H, 3.4, N, 6.7%. ^{1}H NMR (400 MHz, DMSO-*d*$_6$, 298 K, ppm): δ 13.95 (s, 1H, N6–H), 9.48 (d, *J* = 5.8 Hz, 1H, C9–H), 8.54 (d, *J* = 7.9 Hz, 1H, C12–H), 8.23 (t, *J* = 7.9 Hz, 1H, C11–H), 7.67 (m, 5H, C10–H, C28,29–H), 7.16 (s, 1H, C23–H), 6.90 (d, *J* = 9.0 Hz, 1H, C21–H), 6.71 (d, *J* = 9.0 Hz, 1H, C20–H), 6.39 (d, *J* = 5.8 Hz, 1H, C34–H), 6.30 (d, *J* = 5.8 Hz, 1H, C34–H), 6.12 (d, *J* = 5.8 Hz, 1H, C33–H), 6.06 (d, *J* = 5.8 Hz, 1H, C33–H), 4.06 (s, 2H, C15–H), 3.73 (s, 3H, C31–H), 2.56 (sep, *J* = 6.8 Hz, 1H, C37–H), 2.28 (s, 3H, C36–H), 2.19 (s, 3H, C25–H), 1.01–0.96 (m, 6H, C38–H). ^{13}C NMR (101 MHz, DMSO, 298 K, ppm): δ 171.3 (C16), 168.3 (C5), 162.9 (C14), 162.1 (C2), 156.5 (C9–H), 156.0 (C7), 150.1 (C24), 140.8 (C11–H), 138.2 (C30), 136.6 (C17), 134.5 (C27), 131.7–130.7 (C28,29–H), 129.5 (C10–H), 128.6 (C19), 126.1 (C12–H), 115.1 (C21–H), 112.4 (C20–H), 111.8 (C22), 102.4 (C23–H), 96.0 (C32), 95.6 (C35), 78.7 (C34–H), 78.0 (C34–H), 75.5 (C33–H), 74.6 (C33–H), 55.9 (C31–H), 31.0 (C15–H), 30.5 (C37–H), 22.6–22.1 (C38–H), 18.6 (C25–H), 13.9 (C36–H). ESI+ MS (MeOH, *m/z*): 878.1 (calc. 878.1; 100%; [Os(pcym)(L2)Cl]$^+$). IR (ATR, ν, cm^{-1}): 398, 482, 555, 753, 772, 832, 1012, 1033, 1064, 1088, 1144, 1221, 1317, 1354, 1476, 1522, 1606, 1680, 2832, 2871, 2963, 3072, 3319, 3625.

[Os(η^6-pcym)(L3)Cl]PF_6 (**3**): Red solid. Yield: 73%. $C_{35}H_{33}N_4Cl_2F_6O_2OsPS$ (MW = 979.82). Anal. Calc.: C, 42.9, H, 3.4, N, 5.7; found: C, 43.1., H, 3.4, N, 5.4. ^{1}H NMR (400 MHz, DMSO-*d*$_6$, 298 K, ppm): δ 9.51 (d, *J* = 5.9 Hz, 1H, C9–H), 8.61 (d, *J* = 7.9 Hz, 1H, C12–H), 8.27 (t, *J* = 7.9 Hz, 1H, C11–H), 7.79 (t, *J* = 7.9 Hz, 1H, C10–H), 7.70 (m, 4H, C28,29–H), 7.23 (s, 1H, C23–H), 6.93 (d, *J* = 8.6 Hz, 1H, C21–H), 6.78 (d, *J* = 8.6, 1H, C20–H), 6.40 (m, 2H, C34–H), 6.20 (d, *J* = 5.6 Hz, 1H, C33–H), 6.14 (d, *J* = 5.6 Hz, 1H, C33–H), 4.89 (m, 2H, C15–H), 3.72 (s, 3H, C31–H), 2.55 (sep, *J* = 6.8 Hz, 1H, C37–H), 2.41 (s, 3H, C25–H), 2.21 (s, 3H, C36–H), 0.95 (m, 6H, C38–H). ^{13}C NMR (101 MHz, DMSO-*d*$_6$, 298 K, ppm): δ 175.8 (C16), 168.5 (C5), 168.4 (C26), 156.6 (C9–H), 156.2 (C24), 149.0 (C7), 140.8 (C11–H), 138.5 (C30), 136.8 (C17), 134.1 (C27), 131.8–129.6 (C28,29–H), 129.6 (C10–H), 127.5 (C12–H), 115.3 (C21–H), 114.6 (C20–H), 112.3 (C22), 102.0 (C23–H), 96.0 (C32), 95.6 (C35), 79.6 (C34–H), 77.8 (C34–H), 75.8 (C33–H), 74.9 (C33–H), 55.9 (C31–H), 31.0 (C37–H), 25.2 (C15–H), 22.7 (C38–H), 21.8 (C38–H), 18.5 (C25–H), 13.6 (C36–H). ESI+ MS (MeOH, *m/z*): 835.1 (calc. 835.2; 100%;

[Os(pcym)(L3)Cl]$^+$). IR (ATR, ν, cm^{-1}): 378, 482, 555, 662, 688, 753, 831, 926, 1012, 1032, 1062, 1088, 1149, 1223, 1316, 1356, 1400, 1476, 1591, 1679, 2822, 2852, 2923, 2963, 3052, 3647.

General Methods

Electrospray ionization mass spectrometry (ESI-MS; MeOH solutions) was carried out with an LCQ Fleet ion trap spectrometer (Thermo Scientific; Waltham, MA, USA; QualBrowser software, version 2.0.7) in the positive ionization mode (ESI+). ^{1}H and ^{13}C NMR spectroscopy, and ^{1}H-^{1}H gs-COSY, ^{1}H-^{13}C gs-HMQC and ^{1}H-^{13}C gs-HMBC two dimensional (2D) correlation experiments were recorded using $CDCl_3$, DMSO-d_6 or D_2O solutions at 298 K on a Varian spectrometer (Varian Inc.; Palo Alto, CA, USA) at 400.00 MHz (for ^{1}H NMR) and 101.00 MHz (for ^{13}C NMR); gs = gradient selected, COSY = correlation spectroscopy, HMQC = heteronuclear multiple quantum coherence, HMBC = heteronuclear multiple bond coherence. ^{1}H and ^{13}C NMR spectra were calibrated against the residual signals of the used solvents. The splitting of proton resonances in the reported ^{1}H spectra is defined as s = singlet, d = doublet, t = triplet, sep = septet, dd =doublet of doublets and m = multiplet. A Jasco FT/IR-4700 spectrometer (Jasco, Easton, MD, USA) was used for the collection of the Fourier-transform infrared (FTIR) spectra of the studied ligands and complexes in the range of 400–4000 cm^{-1} by using the attenuated total reflection (ATR) technique on a diamond plate. Elemental analysis was performed by a Flash 2000 CHNS Elemental Analyser (Thermo Scientific; Waltham, MA, USA). The molar conductivity measurement was carried out on 1×10^{-3} M solutions of **1**–**3** in methanol, using the Cond 340i/SET device (WTW) at 25 °C. Thermal stability of **1**–**3** was studied using a Discovery SDT 650 thermal analyser for simultaneous thermogravimetry (TG) and differential scanning calorimetry (DSC); TA Instruments; 5 °C/min gradient, air atmosphere 50 mL/min.

In vitro cytotoxicity testing

Cell culture and culture conditions: Selected human tumour and non-tumour cell lines Jurkat (acute T cell leukaemia), MOLT-4 (acute lymphoblastic leukaemia), A549 (lung carcinoma), HT-29 (colorectal adenocarcinoma), PANC-1 (pancreas epithelioid carcinoma), A2780 (ovarian carcinoma), HeLa (cervix adenocarcinoma), MCF-7 (breast adenocarcinoma), SAOS-2 (osteosarcoma) and MRC-5 (normal lung fibroblasts) were purchased from either ATCC (Manassas,

USA) or Sigma-Aldrich (St. Louis, USA) and cultured according to the provider´s culture method guidelines. All cell lines were maintained at 37 °C in a humidified 5% carbon dioxide and 95% air incubator. Cells in the maximum range of either 10 passages for primary cell line (MRC-5), or in the maximum range of 20 passages for cancer cell lines (Jurkat, MOLT-4, A549, HT-29, PANC-1, A2780, HeLa, MCF-7 and SAOS-2) and in an exponential growth phase were used for this study.

Screening of antiproliferative effect and growth percent calculation: Each cell line was seeded at previously established optimal density (1×10^3 to 50×10^3 cells per well) in a 96-well plate (TPP, Trasadingen, Switzerland) and cells were allowed to settle overnight. Cells were treated for 48 h with compounds **1–3** in the final concentration of 10 μM. Doxorubicin (Sigma-Aldrich, St. Louis, USA), at a concentration of 1 μM, was used as a positive control. At the end of the cultivation period, the WST-1 proliferation assay (Roche, Basel, Switzerland) was performed according to the manufacturer´s protocol and the absorbance was measured using a Tecan Spark (Tecan, Männedorf, Switzerland). Each value is the mean of three independent experiments and represents the percentage of proliferation 0.1% DMSO mock-treated control cells (100% cell proliferation). The growth percent (GP) value was calculated for each compound tested. GP represents the mean of the proliferation decrease in percent of all the nine cancer cell lines treated with the same compound.

Growth inhibition assay: The WST-1 (Roche, Mannheim, Germany) reagent was used to determine the effect of complex **3** and doxorubicin against the representative cancer (MCF-7) and non-cancerous (MRC-5) cell lines. The MCF-7 and MRC-5 cells were plated at 1.5×10^3 or 2×10^3, respectively, cells per well in 96-well plates and incubated at 37 °C for 24 h. Both cell lines were treated with **3** at concentrations ranging from 0 to 50 μM. After a 48 h incubation period, 50 μL WST-1 reagent was added. The absorbance was measured after 3 h incubation at 440 nm and reference wavelength 690 nm. The measurement was performed in microplate reader (Tecan Infinite M200 microplate reader; Tecan Group, Männedorf, Switzerland). All experiments were performed in three biological replicates. The IC_{50} values for each cell line were calculated using GraphPad Prism version 6.00 for Windows, GraphPad Software (San Diego, California USA).

Effect of complex 3 on cell cycle progression

After 48 h of treatment with complex **3** (10 μM) or doxorubicin (1 μM), the cells were washed with ice cold PBS and fixed with 70% (v/v) ethanol. In order to detect low molecular-weight

fragments of DNA, the cells were incubated for 5 min at room temperature in a buffer (192 mL 0.2 M Na_2HPO_4 + 8 mL of 0.1 M citric acid, pH 7.8) and then labelled with propidium iodide in Vindelov's solution for 1 h at 37 °C. The DNA content was determined using a CyAn flow cytometer (Beckman Coulter, Miami, FL, USA) with an excitation wavelength of 488 nm. The data were analysed using Multicycle AV software (Phoenix Flow Systems, San Diego, CA, USA).

^{1}H NMR stability studies

The appropriate amounts of complexes **1–3** for the preparation of 1 mM solutions were dissolved in (a) 200 μL of DMSO-d_6 and 300 μL of D_2O or (b) 200 μL of DMSO-d_6 and 300 μL of PBS in D_2O (pH 7.4) or (c) 200 μL of DMF-d_7 and 300 μL of PBS in D_2O (pH 7.4). The prepared solutions were analysed by ^{1}H NMR spectroscopy at various time points (0–48 h) and incubated at ambient temperature between the individual experiments. The obtained ^{1}H NMR spectra were referenced to the residual signal of H_2O (4.79 ppm). The stability of **1–3** was evaluated by integrating the representative ^{1}H NMR resonance of the C9–H hydrogen. *Note*: The used organic solvents (DMSO-d_6, DMF-d_7) ensured the solubility of the tested complexes, as their solubility in water is very low.

^{1}H NMR spectra were also acquired for dehalogenated **1*–3*** species, which were prepared from the fresh solutions of **1–3** in 40% DMSO-d_6/60% D_2O by the addition of the stoichiometric amount of silver nitrate. The mixtures were shaken under an aluminium foil (25 °C) for 1 h, then the formed precipitate of AgCl was centrifuged (5 min, 11,000 rpm) and the obtained solutions were used for ^{1}H NMR experiments.

Interaction with biomolecules

Reduced glutathione: GSH (5 mol equiv.) was added to the solutions of complexes **1–3** (1 mM) in 200 μL of DMF-d_7 and 300 μL of PBS in D_2O (pH 7.4). ^{1}H NMR spectra of the prepared solutions were recorded at various time points (0–48 h) and incubated at ambient temperature between the individual experiments. Similar experiment was performed for **1–3** in 800 μL of MeOH and 1,200 μL of PBS in H_2O (pH 7.4) and analysed by ESI+ MS at various time points (0–24 h; incubated at ambient temperature between the individual experiments).

NADH: An excess of NADH (5 mol equiv.) was added to complexes **1–3** (1 mM final concentration) dissolved in 200 μL of DMSO-d_6 and 300 μL of PBS in D_2O (pH 7.4) and in 200 μL of

DMF-d_7 and 300 μL of PBS in D_2O (pH 7.4). The prepared solutions were analysed by ^1H NMR at various time points (0–48 h) and incubated at ambient temperature between the measurements.

GMP: GMP (1 mol equiv.) was dissolved in 300 μL of PBS in D_2O and these solutions were added to **1** and **3** (1 mM final concentration) in 200 μL of DMSO-d_6 or 200 μL of DMF-d_7 mixed with 300 μL of PBS in D2O (final pH 7.4 for both mixtures of solvents). ^1H NMR spectra were recorded at various time points (0–72 h) and the solutions were incubated at ambient temperature between the individual experiments.

Carboxypeptidase A: An interaction of complex **2** with the carboxypeptidase A from bovine pancreases (CAP A) was investigated by ESI+ mass spectrometry in order to follow the possible release of the ind substituent. For these advanced experiments, CAP A (10 units) was dissolved in 1,200 μL of PBS in H_2O (pH 7.4) and this solution was mixed with an appropriate amount of **2** (10 μM final concentration) in 800 μL of MeOH. The mixture was analysed at various time points (0–24 h) and incubated at ambient temperature between the experiments. Similar experiment was carried out by reversed-phase high-performance liquid chromatography (RP-HPLC) coupled to ESI+ MS by the UHPLC-MS device (Dionex/Thermo Fisher Scientific) equipped with an Acclaim 120 (C18 stationary phase; 5 μm pore size, 120 Å, 2.1 × 50 mm). The mixture of 0.01 M ammonium formate in H_2O (A) and MeCN (B) was used as the mobile phase at gradients of 10 % B (t = 0 min), 75 % B (t = 15 min), 75 % B (t = 20 min), 10 % B (t = 21 min) and 10 % B (t = 30 min) over a 30 min period (0.4 mL min^{-1} flow rate). The detection wavelength was 254 nm. Complex **1** and free indomethacin were involved in the HPLC/ESI+ MS studies for comparative purposes.

Studies of lipophilicity (log P)

Octanol-saturated water (OSW) and water-saturated octanol (WSO) were prepared from octanol and 0.2 M water solution of KCl by the overnight stirring. The stock solutions were pre-pared by shaking of 1 μmol of complexes **1**–**3** in 11 mL of OSW for 1 h. Then the mixtures were centrifuged (5 min, 11,000 rpm) and supernatant was collected. 5 mL of this solution was studied by ICP-MS, while other 5 mL of this solution was added to 5 mL of WSO and shaken for 2 h at ambient temperature. After that, these mixtures were centrifuged (5 min, 11,000 rpm), and aqueous layers were carefully separated. The Os concentrations were deter-mined by ICP-MS (the obtained value was corrected for the adsorption effects). log P = log([M]WSO/[M]OSW_a) equation was used for the

partition coefficient calculation, where $[M]OSW_b$ and $[M]OSW_a$ stands for the Os concentration before and after partition, respectively, and $[M]WSO = [M]OSW_b - [M]OSW_a$.

Results

Synthesis of L1–L3

5-(Pyridin-2-yl)-1,3,4-thiadiazol-2-amine (L1) was prepared by a known cyclisation reaction of 2-pyridinecarbonitrile with thiosemicarbazide in trifluoroacetic acid in a moderate yield.[2] Activation of carboxylic group of Hind with carbonyldiimidazole (CDI) and subsequent reaction with the amide precursor L1 reproducibly yielded the ind-functionalized derivative L2 in moderate-high yields, with indomethacin conjugated to the thiadiazole moiety through the amide bond (Scheme 1). It is worth noting that we used excess of Hind in order to ensure the complete consumption of L1. Final pH adjustment with aq. ammonia created the soluble ammonium salt of unreacted indomethacin, thus only the insoluble derivative L2 precipitated out. The derivative L3 was of a different design (aliphatic linker) and it was prepared for comparative purposes. Compounds L1–L3 were identified by ^{1}H NMR (Figures S1–S3), ^{13}C NMR (Figures S4–S6) and 2D NMR experiments (^{1}H–^{1}H COSY, ^{1}H–^{13}C HMQC, ^{1}H–^{13}C HMBC; Figures S7–S15).

NMR of L1–L3

^{1}H NMR spectrum of L1 contained the characteristic resonances of C9–H and C12–H of pyridine at 8.54 ppm and 8.01 ppm, respectively. After the ind substitution, these signals appeared at 8.63 and 8.17 ppm, respectively, for L2, and at 8.60 and 8.18 ppm, respectively, for L3. The signal of the amine group of L1 (δ = 7.49 ppm) shifted significantly to lower fields (δ = 12.94 ppm), with appropriate integral intensity decrease, as a consequence of the amide bond formation for the functionalized derivative L2. Further, the ^{1}H NMR spectra of the ind-based derivatives L2 and L3 contained the characteristic singlets of the methyl and methoxy groups of the ind substituent, which were detected at 2.27/2.49 ppm and 3.72/3.79 ppm for L2 and L3, respectively.

NMR of 1–3

For the ^{1}H NMR and ^{13}C NMR spectra of **1**–**3** (ESI, Fig. S18–S32†), the characteristic resonances of methyl groups of the η^{6}-coordinated *p*-cymene were detected at *ca* 2.15 and 0.85 ppm (for ^{1}H NMR), and 13.9 and 18.6 ppm (for ^{13}C NMR). Regarding ^{13}C NMR spectra, besides the mentioned pcym signals, other characteristic resonances were detected and assigned to the building blocks of the L1–L3 ligands. The presence of the ind substituent in the structure of **1**–**3** was unambiguously proved by the detection of characteristic ^{13}C NMR resonances of its methyl group at 18.6 ppm (for **2**) and 18.5 ppm (for **3**). Importantly, the –*C*H$_2$– ^{13}C NMR resonance of the acetamide (δ = 31.0 for **2**) and methylene (δ = 25.2 ppm for **3**) linkers was also detected in the ^{13}C NMR spectra of the mentioned complexes. The highest ^{13}H NMR coordination shifts of **1**–**3** were calculated for C6 and C12 carbon atoms of the pyridine ring of the used ligands L1–L3 (ESI, Table S1†).

FTIR spectroscopy

The FTIR spectra of complexes **2** and **3** contained the bands of the ν(C=O) vibration at *ca.* 1680 cm^{-1}, which was not detected for complex **1**, thus proved the presence of ind substituent in their structure.[4] In addition, spectra of **1** and **2** showed an intensive band of the ν(N–H) vibration at *ca.* 3400 cm^{-1}, characteristic for the amino group, which was not detected for the amine-free complex **3**. This chemical difference between **2** and **3** (i.e. the presence of the amide bond for **2**) was also connected with the characteristic peak of the δ(NH) vibration, which was detected only for **2** (1556 cm^{-1}). Between 2800 cm^{-1} and 3100 cm^{-1}, bands of the ν(C–H) vibrations of aromatic and aliphatic C–H groups were observed. The characteristic peaks of the thiadiazole ring (ν(C=S) vibration at *ca* 1060 cm^{-1}) were also detected in the obtained spectra of complexes **1**–**3**.[5] Finally, the bands centred at *ca.* 555 and 830 cm^{-1} are assignable to the vibrations of the PF_6^- counterion (Figure S20).[6] Broad peaks at 3625–3647 cm^{-1} are not assignable to the used ligands (i.e., L1–L3 and pcym) and most likely belong to the vibrations of water moisture.[7] The coordination of a {Os(η^{6}-pcym)Cl } moiety to L1–L3 was connected with the detection of a peak at 1591–1606 cm^{-1}. This is best exemplified for **1**, because the characteristic υ(CN) peak of free L1 (1639 cm^{-1}), which is not overlapped with υ(C=O) as in the case of ind-containing complexes **2** and **3**, shifted markedly after the coordination of this ligand to the structure of **1** (1606 cm^{-1}).

References

[1] P. Štarha, Z. Trávníček, J. Vančo and Z. Dvořák, *Molecules*, 2018, **23**, 420 (16 pages).

[2] W. Xue, X. Li, G. Ma, H. Zhang, Y. Chen, J. Kirchmair, J. Xia and S. Wu, *Eur. J. Med. Chem.*, 2020, **188**, 112022 (18 pages).

[3] (*a*) P. Zoufalý, E. Čižmár, J. Kuchár and R. Herchel, *Molecules*, 2020, **25**, 277 (18 pages); (*b*) B. Gierczyk and M. Zalas, *Org. Prep. Proced. Int.*, 2005, **37**, 213–222.

[4] H. M. Badawi and W. Forner, *Spectrochim. Acta A*, 2014, **123**, 447–454.

[5] T. A. Mohamed, U. A. Soliman, I. A. Shaaban, W. M. Zoghaib and L. D. Wilson, *Spectrochim. Acta A*, 2015, **150**, 339–349.

[6] P. Govindaswamy, Y. A. Mozharivskyj and M. R. Kollipara, *Polyhedron*, 2005, **24**, 1710–1716.

[7] F. Perakis, L. De Marco, A. Shalit, F. Tang, Z. R. Kann, T. D. Kühne, R. Torre, M. Bonn and Y. Nagata, *Chem. Rev.*, 2016, **116**, 7590–7607.

Table S1. Selected ^{1}H and ^{13}C NMR coordination shifts (Δδ; ppm) calculated for complexes **1**–**3** ($\Delta\delta = \delta_{complex} - \delta_{ligand}$).

Resonance	**1**	**2**	**3**
^{1}H NMR			
C9–*H*	0.90	0.85	0.91
C10–*H*	0.38	0.19	0.27
C11–*H*	0.44	0.28	0.04
C12–*H*	0.20	0.37	0.07
C15–H_2	–	0.10	0.30
^{13}C NMR			
*C*9	6.0	6.5	6.5
*C*10	3.5	4.1	3.7
*C*11	3.3	3.0	2.9
*C*12	5.8	6.2	7.3
*C*15	–	0.4	0.8

Table S2. The *in vitro* cytotoxicity results for Os(II) complexes **1**–**3** (10 μM concentration) and the reference drug doxorubicin (1 μM concentration) against human Jurkat (acute T cell leukemia), MOLT-4 (acute lymphoblastic leukemia), A549 (lung carcinoma), HT-29 (colorectal adenocarcinoma), PANC-1 (pancreas epithelioid carcinoma), A2780 (ovarian carcinoma), HeLa (cervix adenocarcinoma), MCF-7 (breast adenocarcinoma), SAOS-2 (osteosarcoma) and MRC-5 (normal lung fibroblasts) cell lines (48 h exposure, WST-1 proliferation assay). The growth percent (GP) value was calculated for each tested compound as the mean of the proliferation change (in percent) of all the nine cancer cell lines (*i.e.*, the non-cancerous MRC-5 cells were excluded from these calculations) treated with the tested compound.

Cell line	Proliferation (%±SD)			
	Complex **1**	Complex **2**	Complex **3**	Doxorubicin
Jurkat	102±16	98±12	106±19	3±0
MOLT-4	110±11	109±15	128±4	5±4
A549	122±13	118±26	107±12	21±11
HT-29	109±10	93±5	104±15	57±14
PANC-1	112±17	112±12	108±8	90±9
A2780	106±9	115±9	89±15	7±2
HeLa	102±6	86±7	68±2	20±9
MCF-7	104±6	108±9	60±13	40±5
SAOS-2	106±14	100±7	96±8	89±13
MRC-5	147±1	137±3	127±6	32±10
GP	108±6	104±11	96±21	37±35

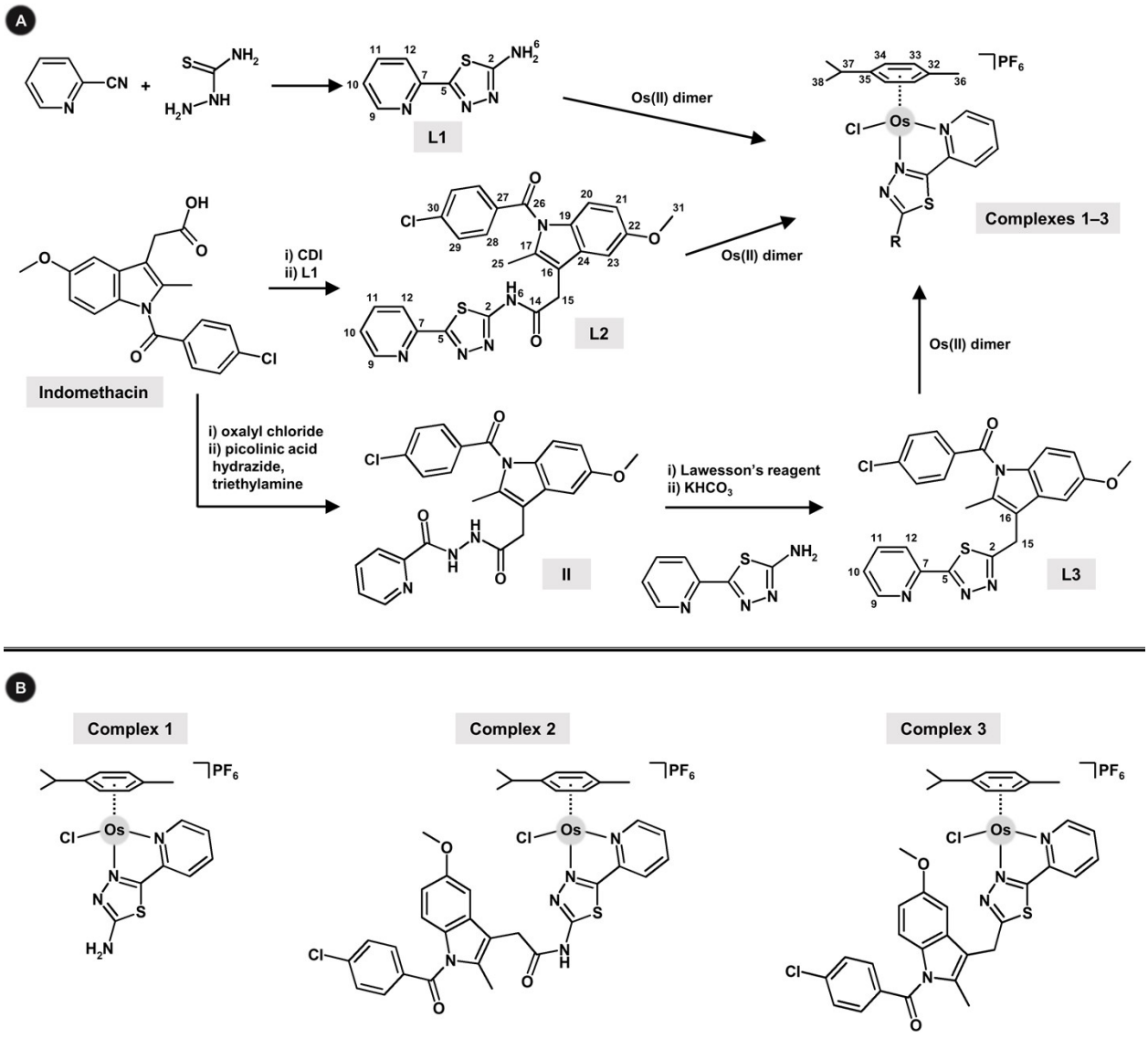

Scheme S1. (***A***) Preparation of thiadiazole-based derivatives 5-(pyridin-2-yl)-1,3,4-thiadiazol-2-amine (L1), 1-(4-chlorobenzoyl)-5-methoxy-2-methyl-1*H*-indol-3-yl)-*N*-(5-(pyridin-2-yl)-1,3,4-thiadiazol-2-yl)acetamide (L2), (4-chlorophenyl){5-methoxy-2-methyl-3-[(5-(pyridin-2-yl)-1,3,4-thiadiazol-2-yl)methyl]-1*H*-indol-1-yl}methanone (L3) and their Os(II) complexes **1**–**3**. CDI = carbonyldiimidazole, Os(II) dimer = $[Os(\mu\text{-}Cl)(\eta^6\text{-pcym})Cl]_2$ (pcym = *p*-cymene). (***B***) Structural formulas of the studied Os(II) complexes $[Os(\eta^6\text{-pcym})(L1)Cl]PF_6$ (**1**), $[Os(\eta^6\text{-pcym})(L2)Cl]PF_6$ (**2**) and $[Os(\eta^6\text{-pcym})(L3)Cl]PF_6$ (**3**).

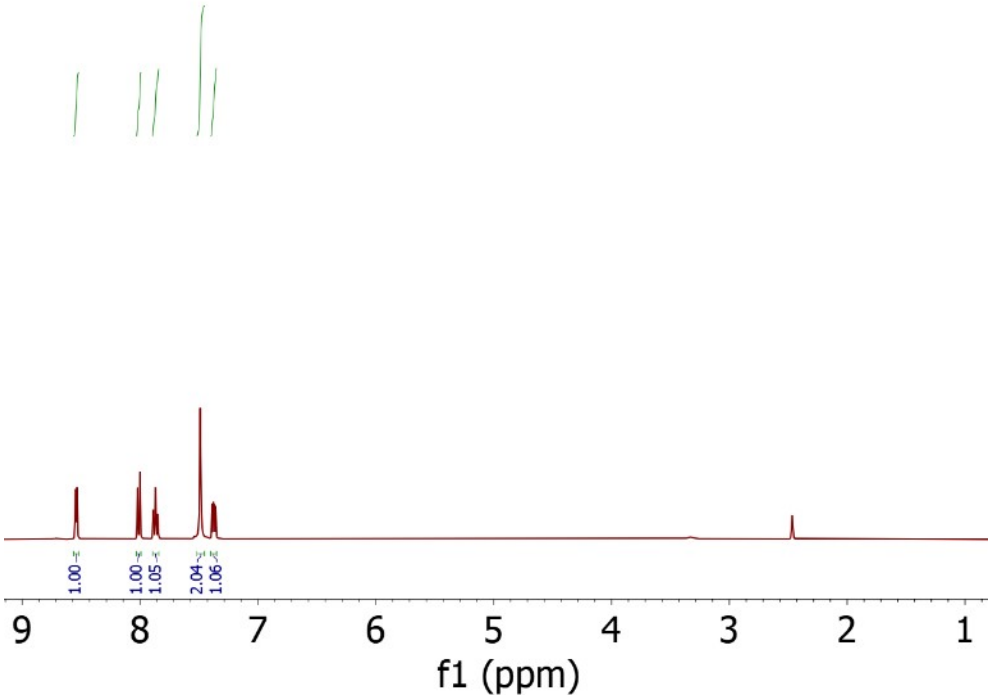

Figure S1. ^{1}H NMR spectra of compound L^{1} (dissolved in DMSO-d_6).

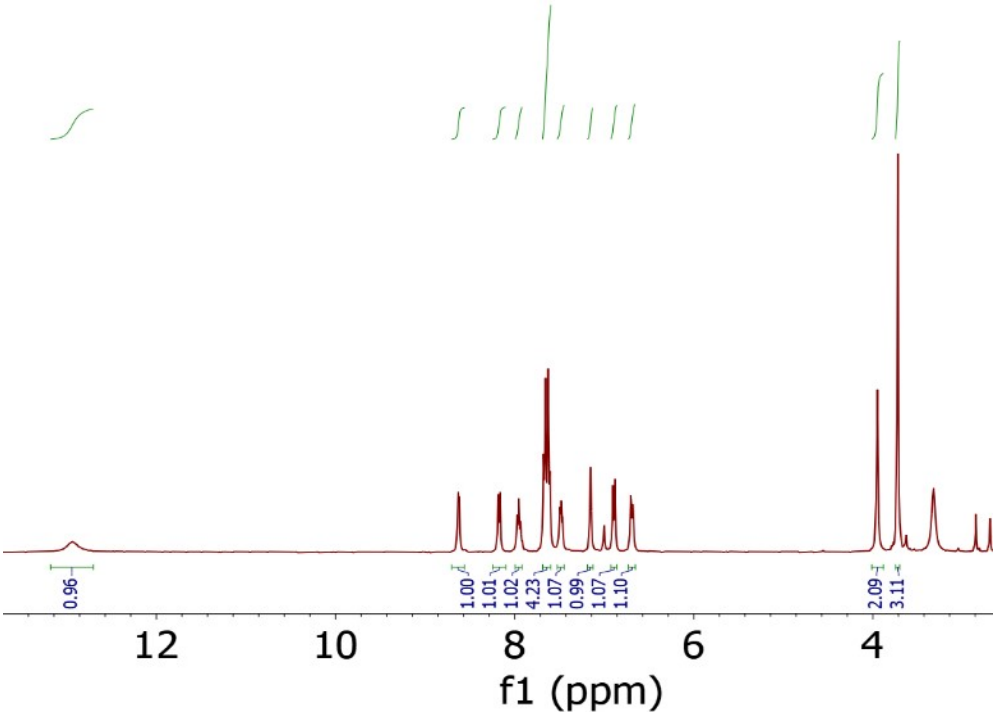

Figure S2. ^{1}H NMR spectra of compound L^{2} (dissolved in DMSO-d_6).

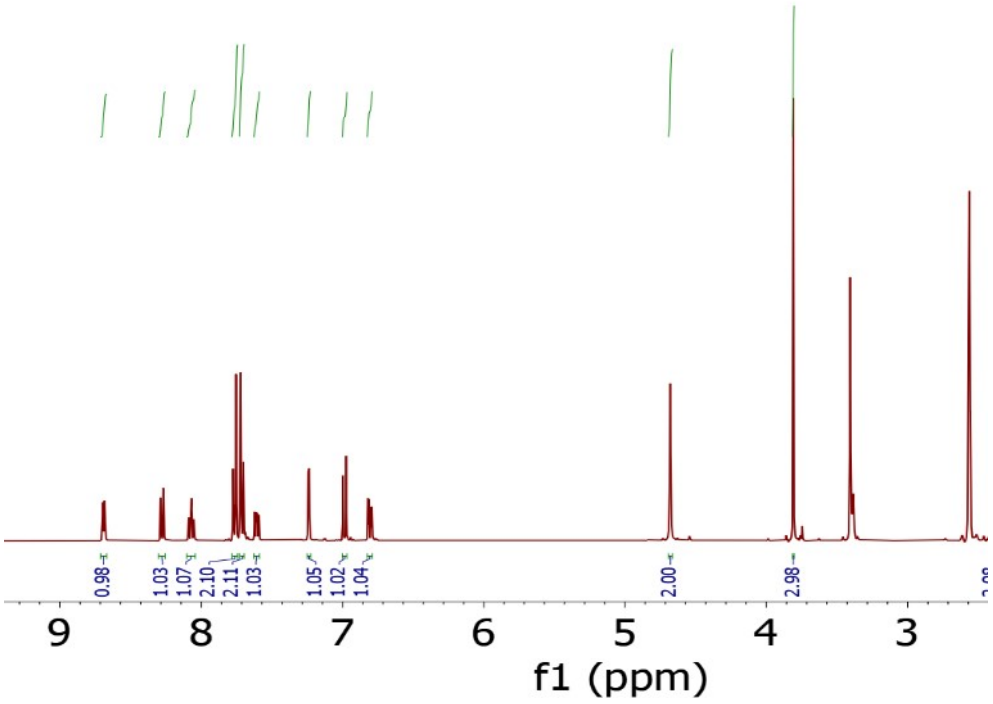

Figure S3. ^{1}H NMR spectra of compound L^{3} (dissolved in DMSO-d_6).

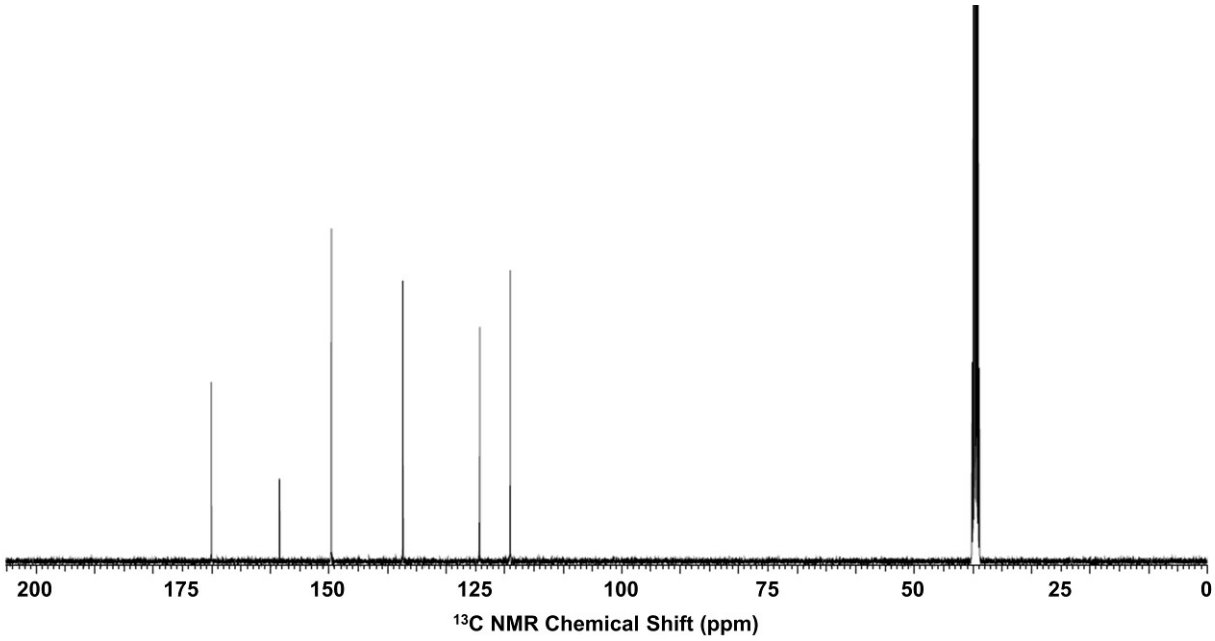

Figure S4. ^{13}C NMR spectra of compound L^1 (dissolved in DMSO-d_6).

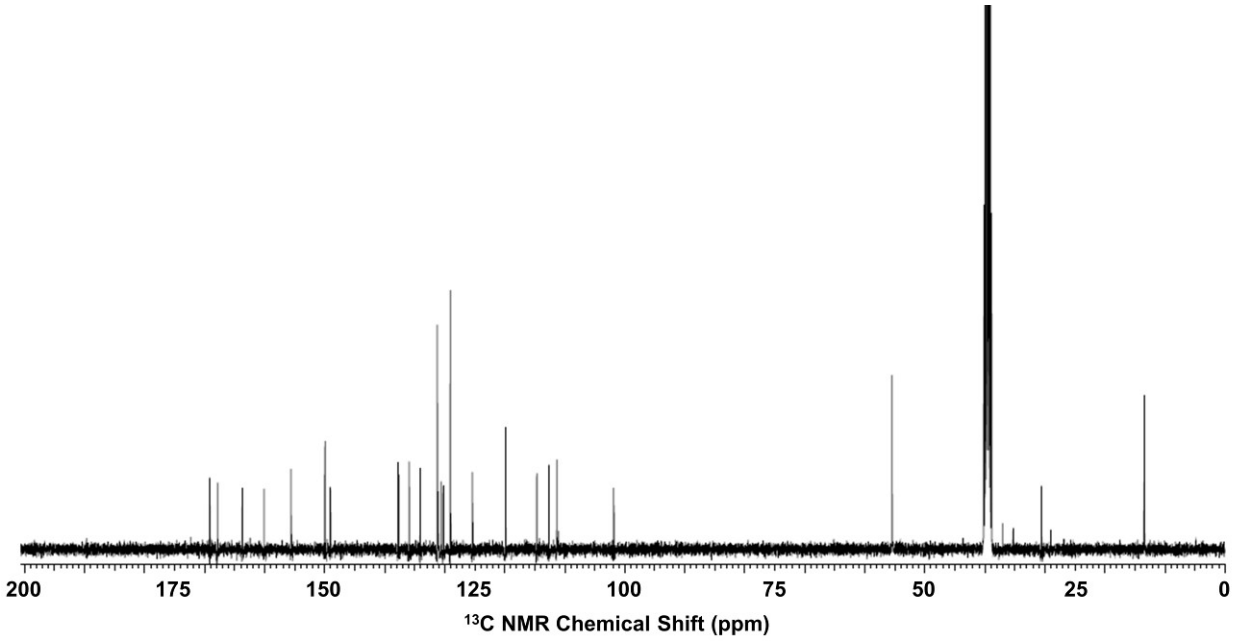

Figure S5. ^{13}C NMR spectra of compound L^2 (dissolved in DMSO-d_6).

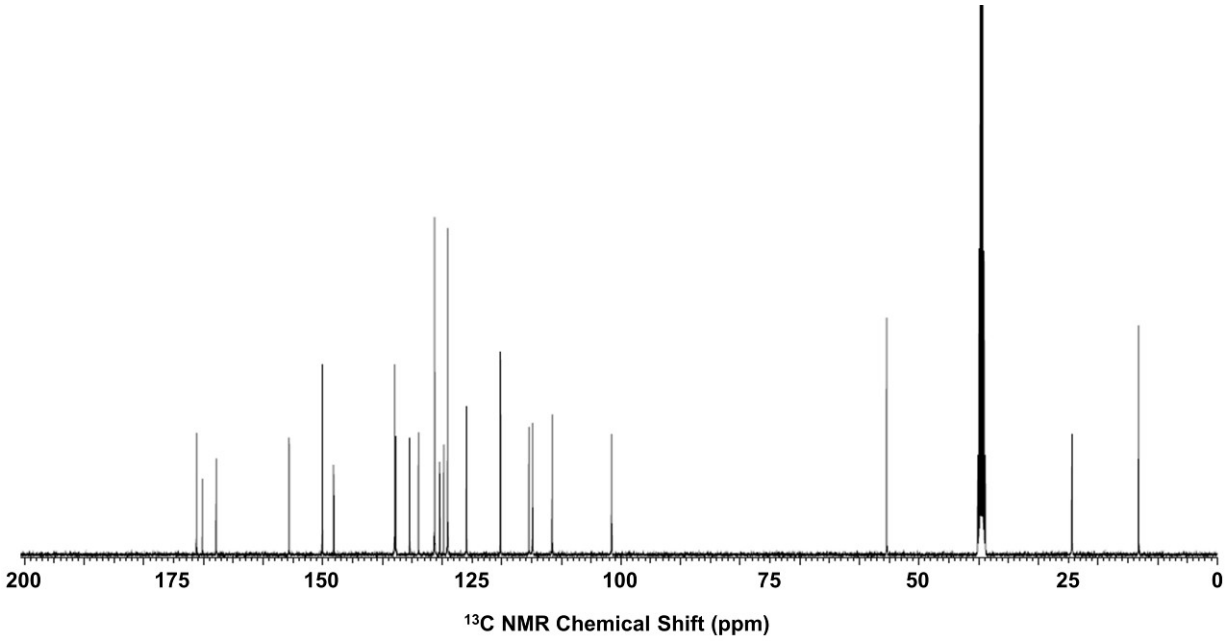

Figure S6. ^{13}C NMR spectra of compound L^3 (dissolved in DMSO-d_6).

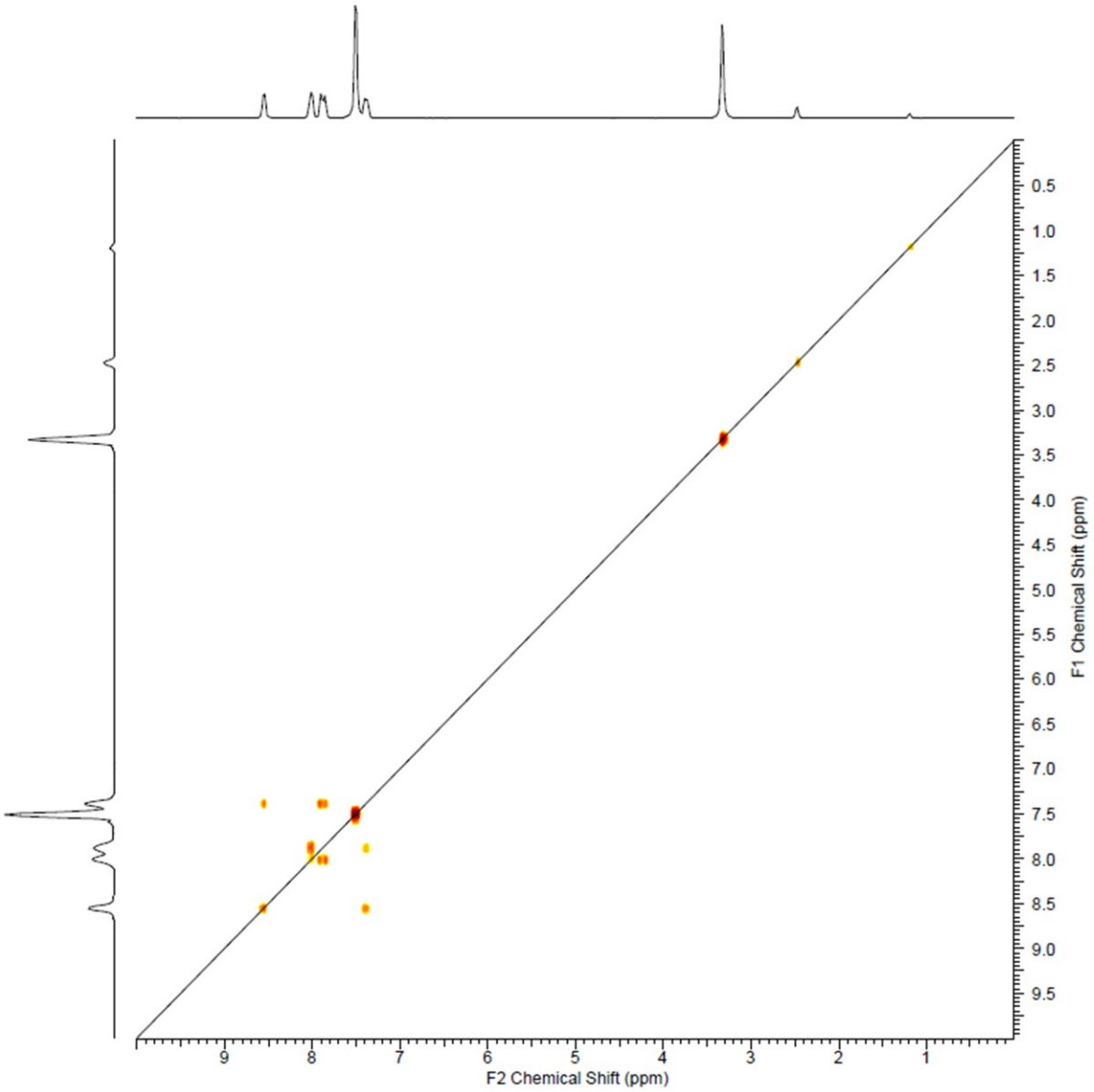

Figure S7. $^{1}H–^{1}H$ COSY spectrum of compound L^{1} (dissolved in DMSO-d_6).

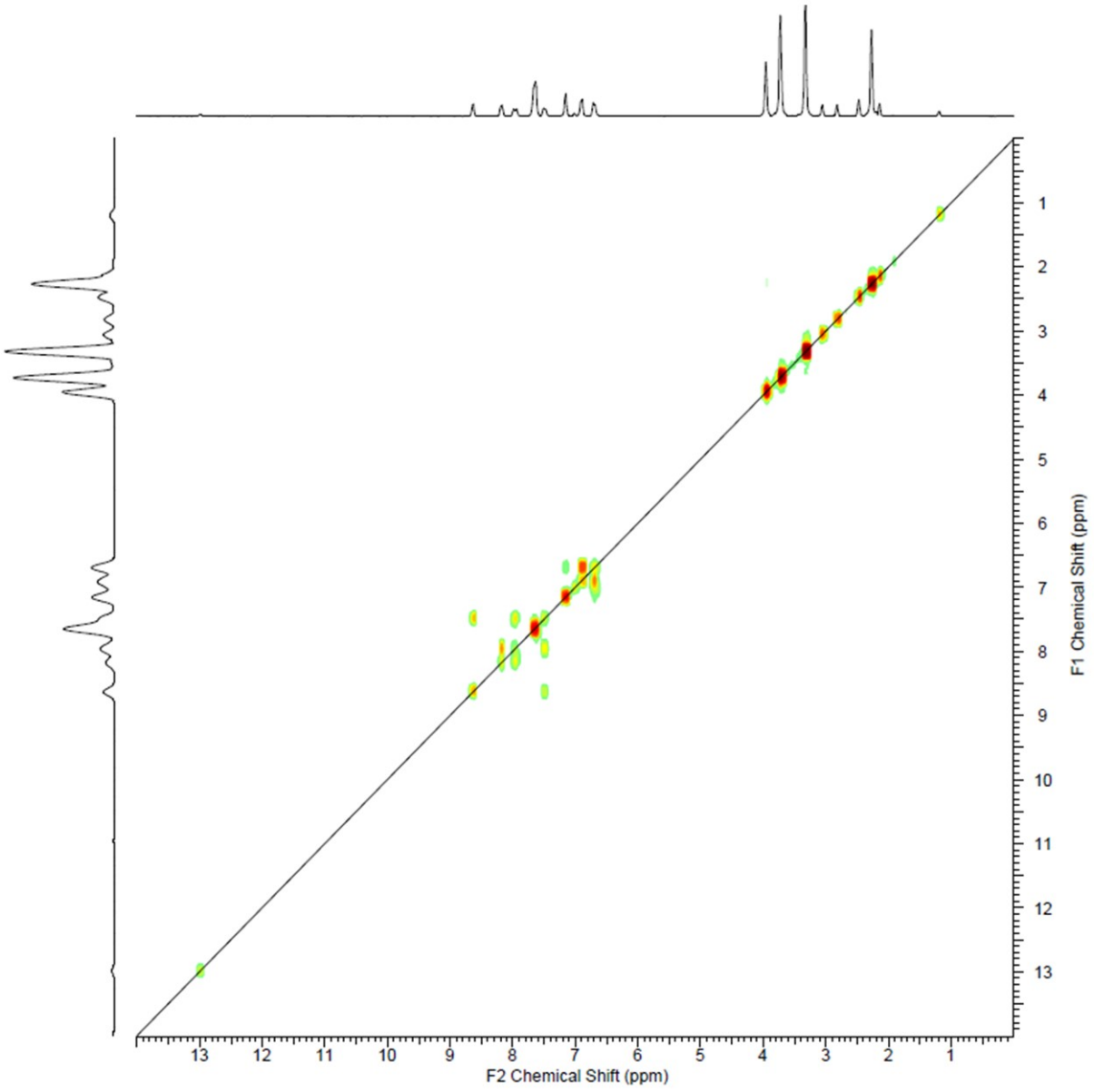

Figure S8. $^{1}H–^{1}H$ COSY spectrum of compound L^{2} (dissolved in DMSO-d_6).

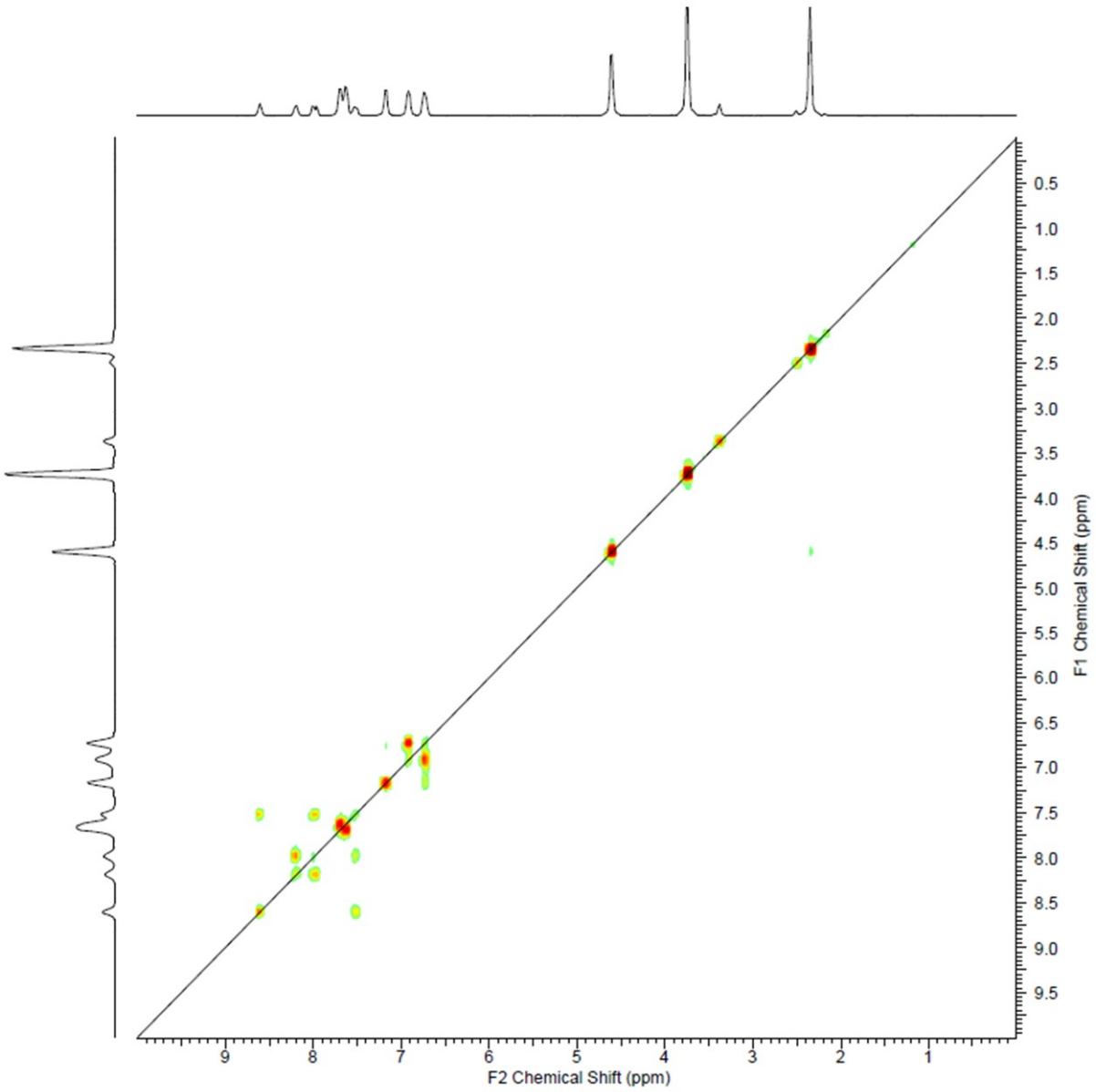

Figure S9. $^{1}H–^{1}H$ COSY spectrum of compound L^{3} (dissolved in DMSO-d_6).

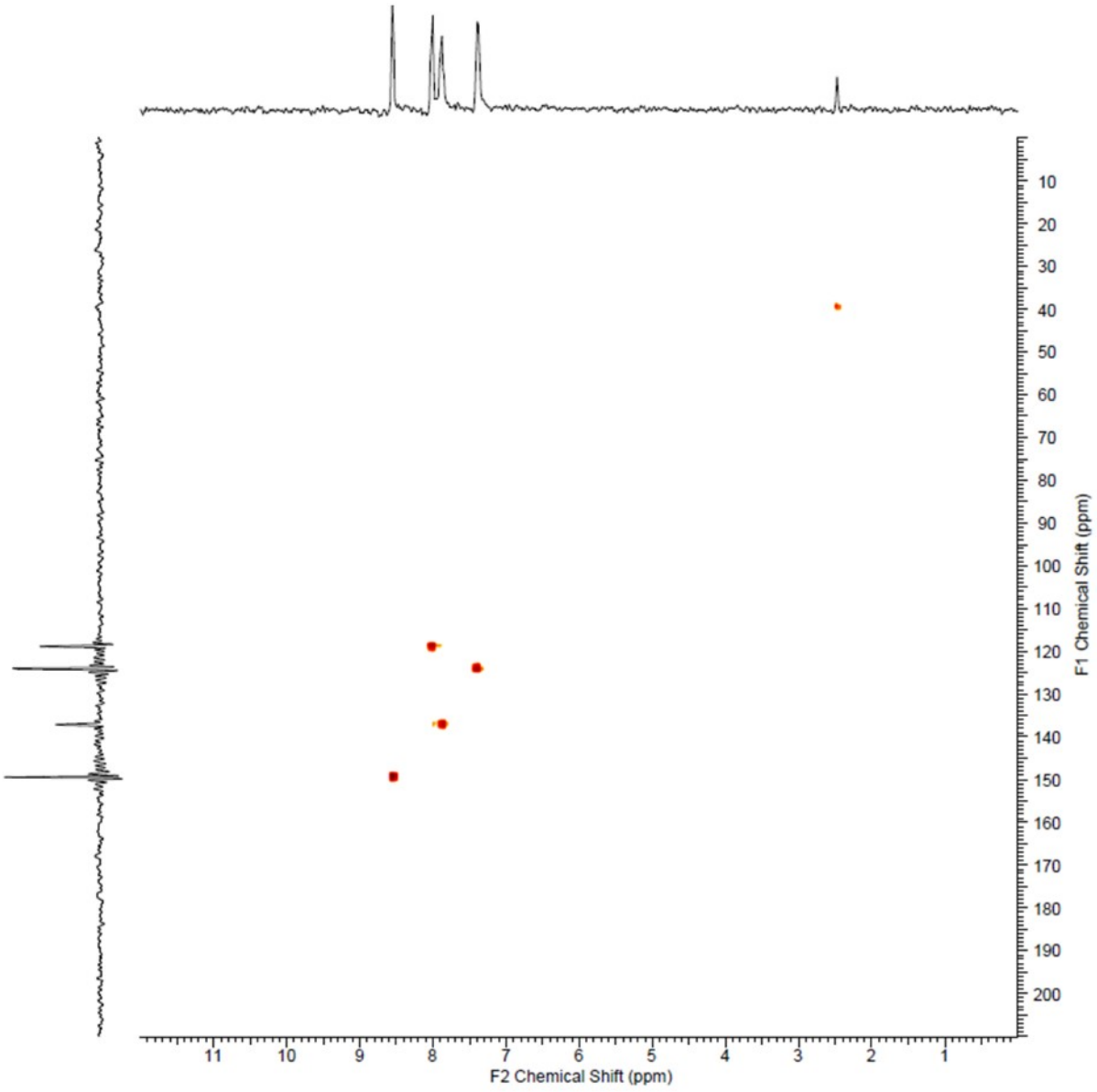

Figure S10. $^{1}H–^{13}C$ HMQC spectrum of compound L^{1} (dissolved in DMSO-d_6).

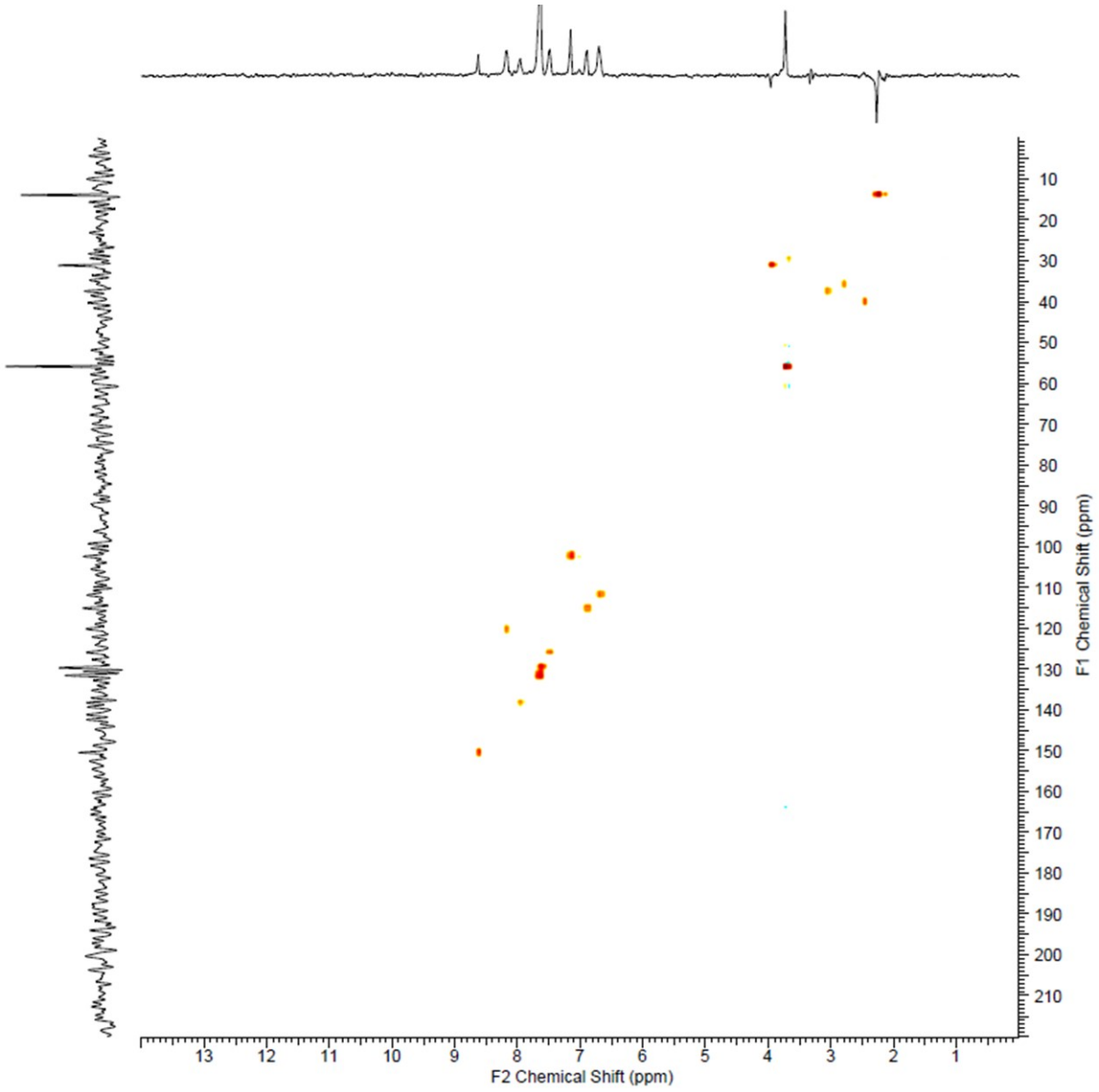

Figure S11. $^{1}H–^{13}C$ HMQC spectrum of compound L^2 (dissolved in DMSO-d_6).

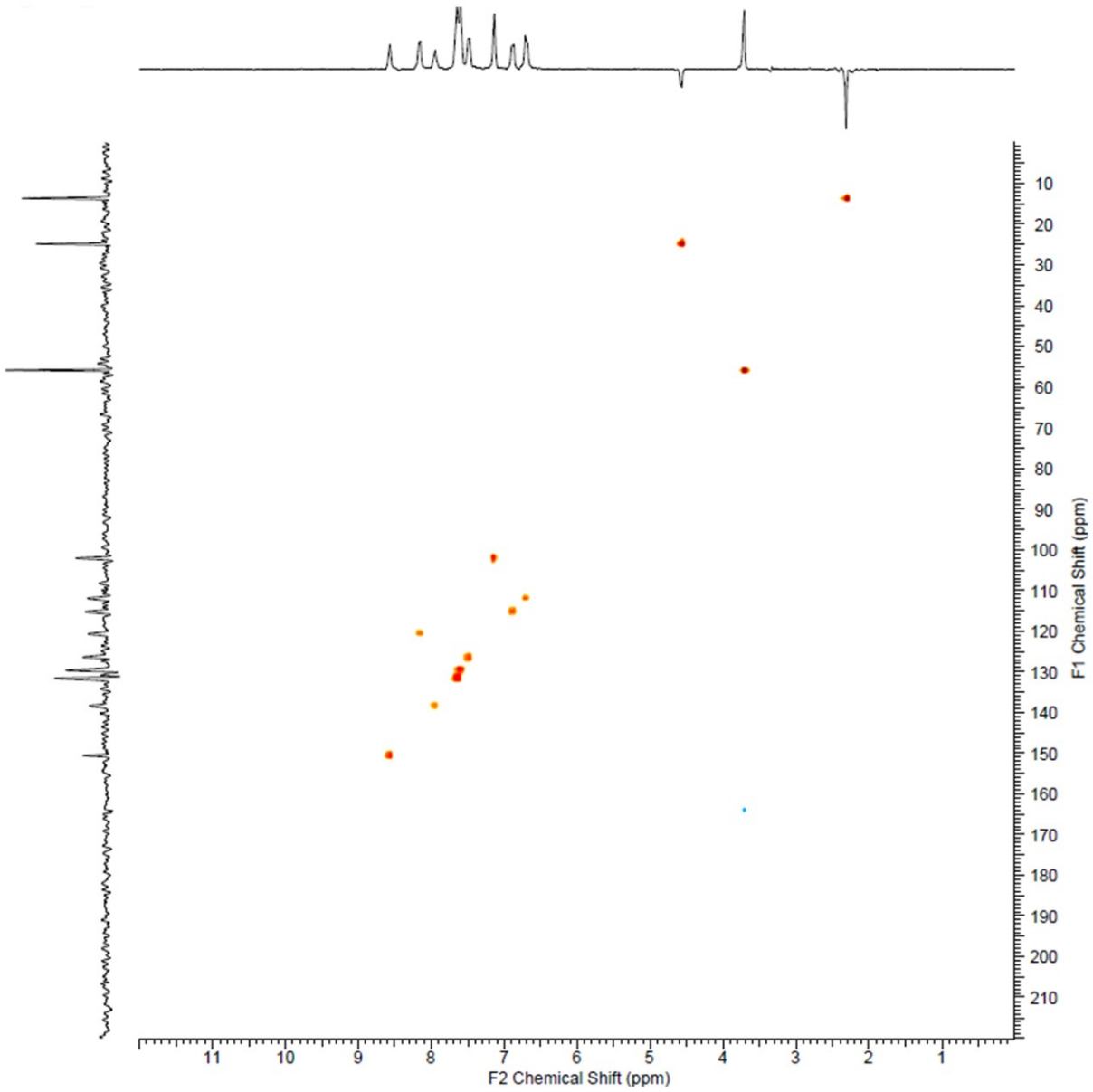

Figure S12. $^{1}H–^{13}C$ HMQC spectrum of compound L^3 (dissolved in DMSO-d_6).

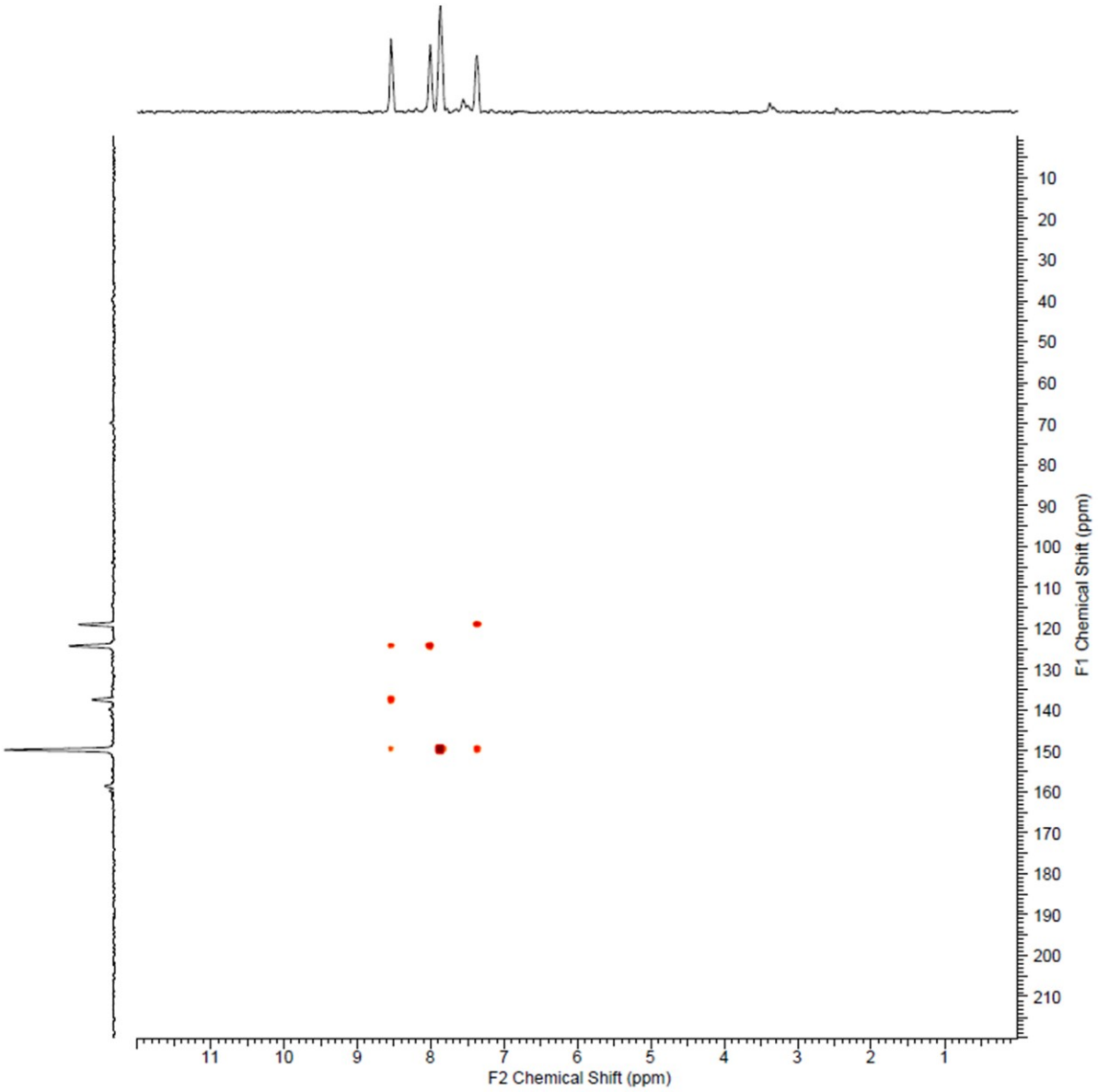

Figure S13. $^{1}H–^{13}C$ HMBC spectrum of compound L^{1} (dissolved in DMSO-d_6).

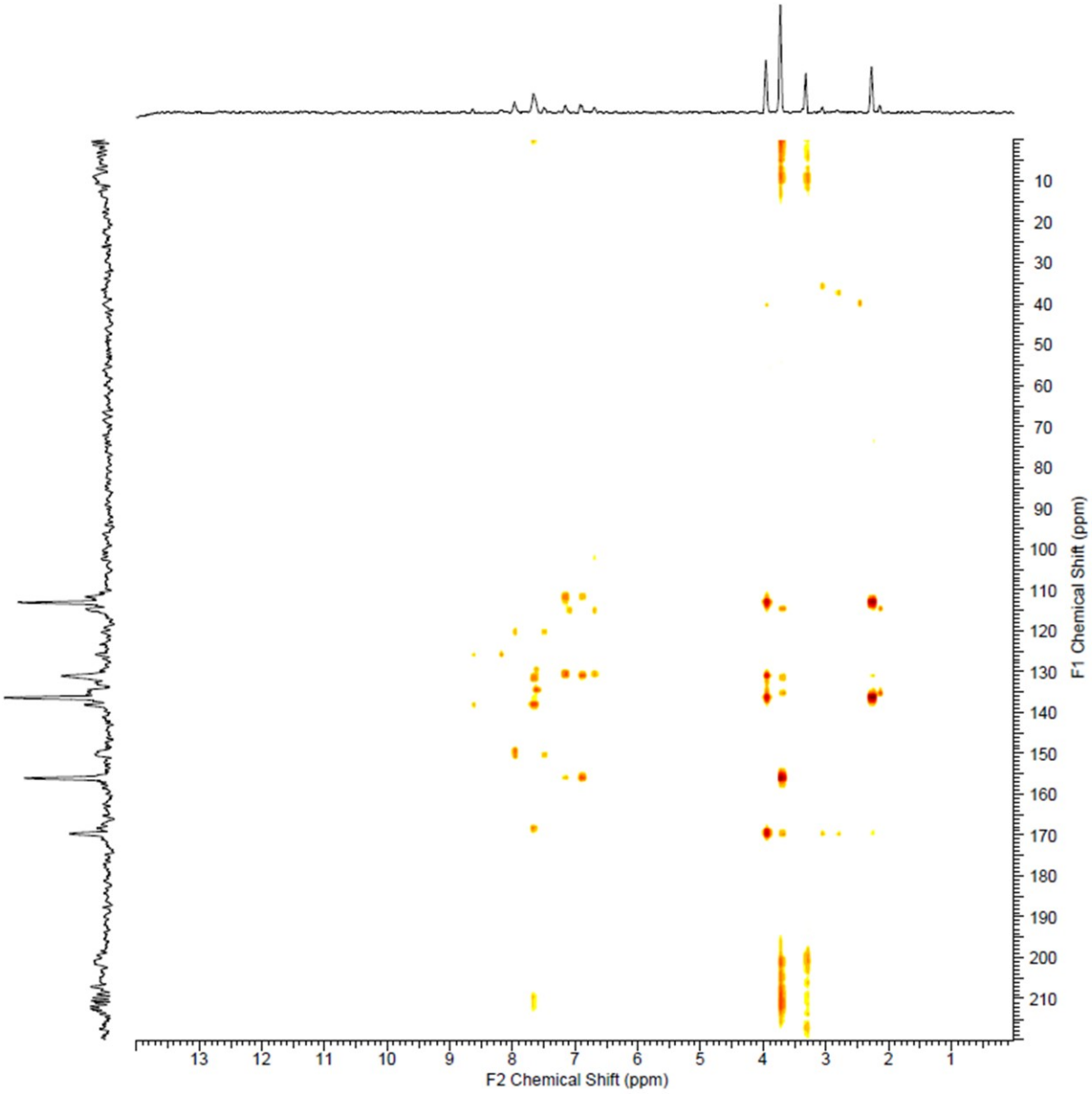

Figure S14. $^{1}H–^{13}C$ HMBC spectrum of compound L^2 (dissolved in DMSO-d_6).

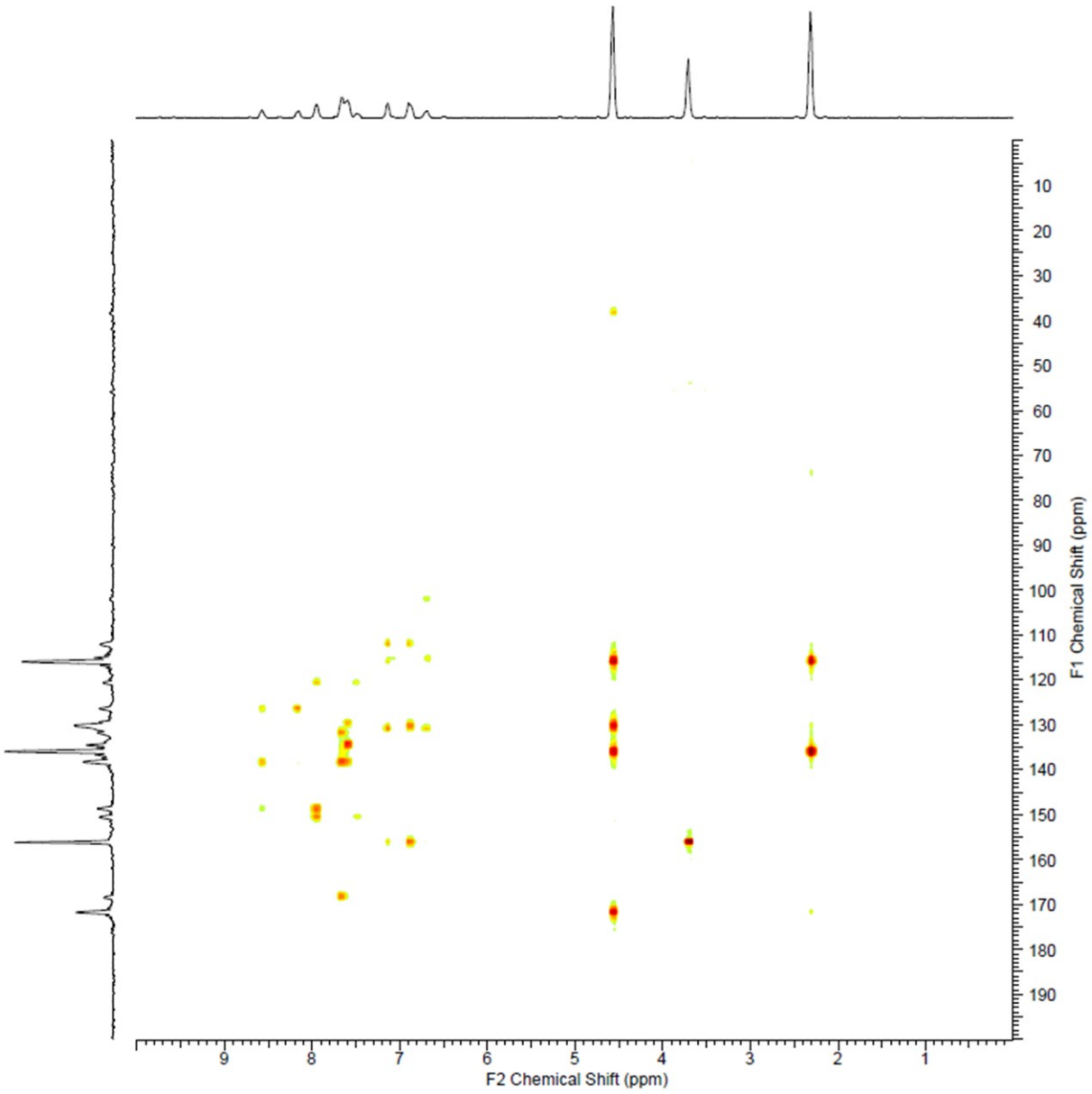

Figure S15. $^{1}H–^{13}C$ HMBC spectrum of compound L^3 (dissolved in DMSO-d_6).

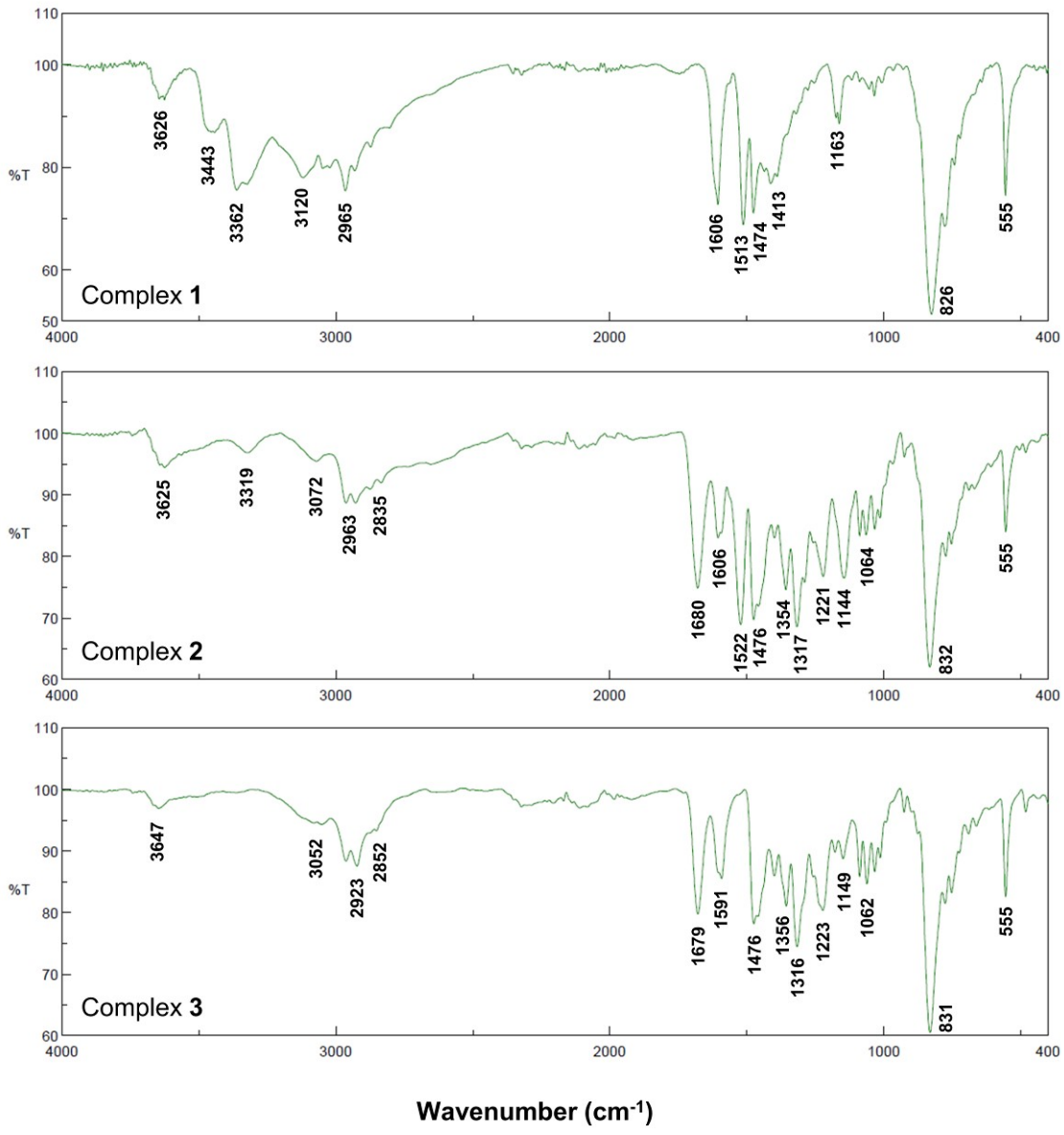

Figure S16. FTIR spectra of compounds **1** (*top*), **2** (*middle*) **3** (*bottom*); ATR technique.

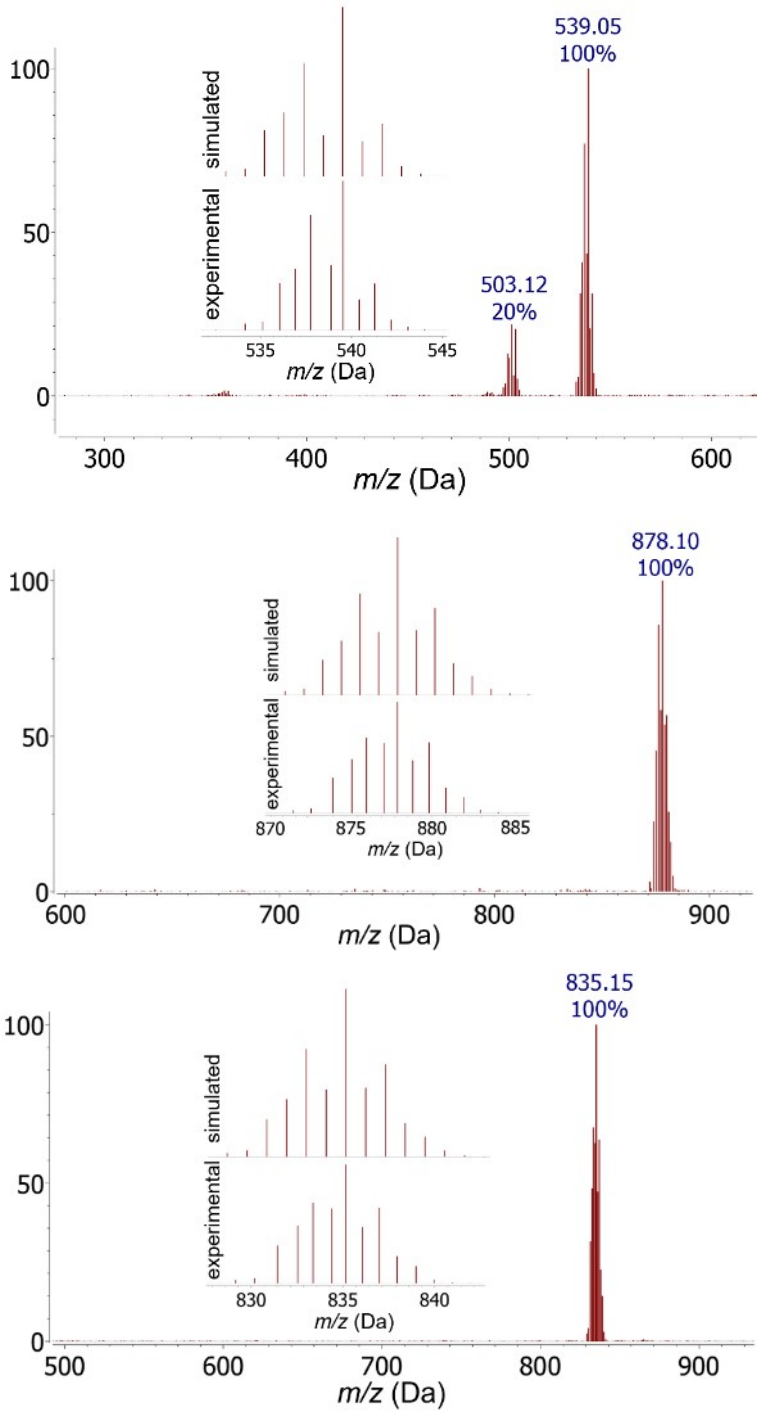

Figure S17. ESI+ mass spectra of **1**–**3** (in MeOH), given with details of both the experimental (*inset bottom*) and simulated (*inset top*) isotopic pattern of the $[M(ar)(L^n)Cl]^+$ species; ESI+ = positive electrospray ionization mode.

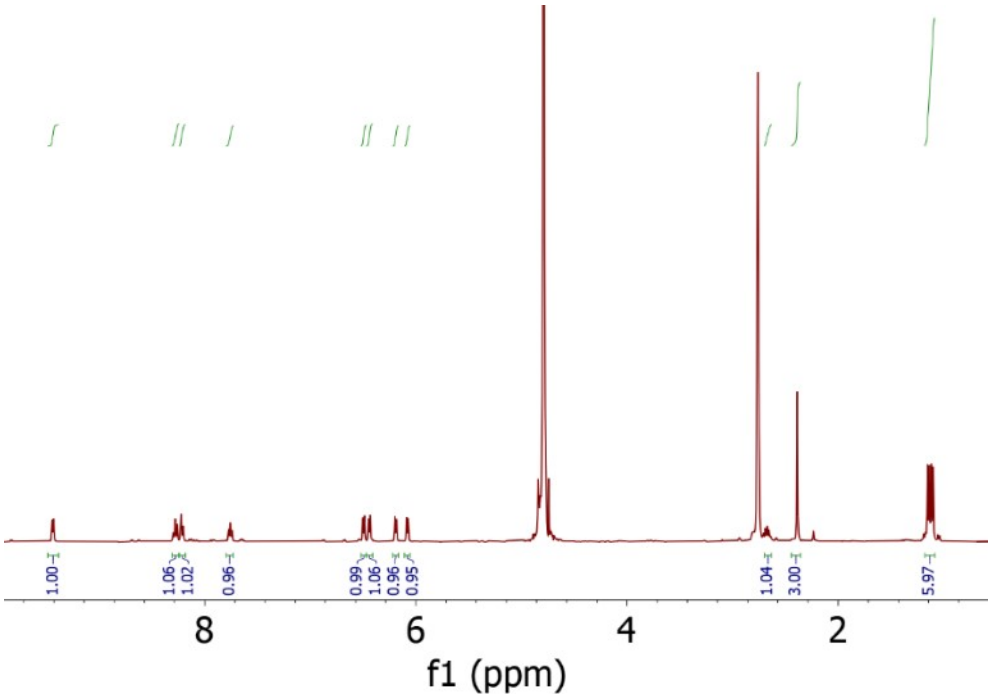

Figure S18. ^{1}H NMR spectrum of complex **1** in DMSO-d_6.

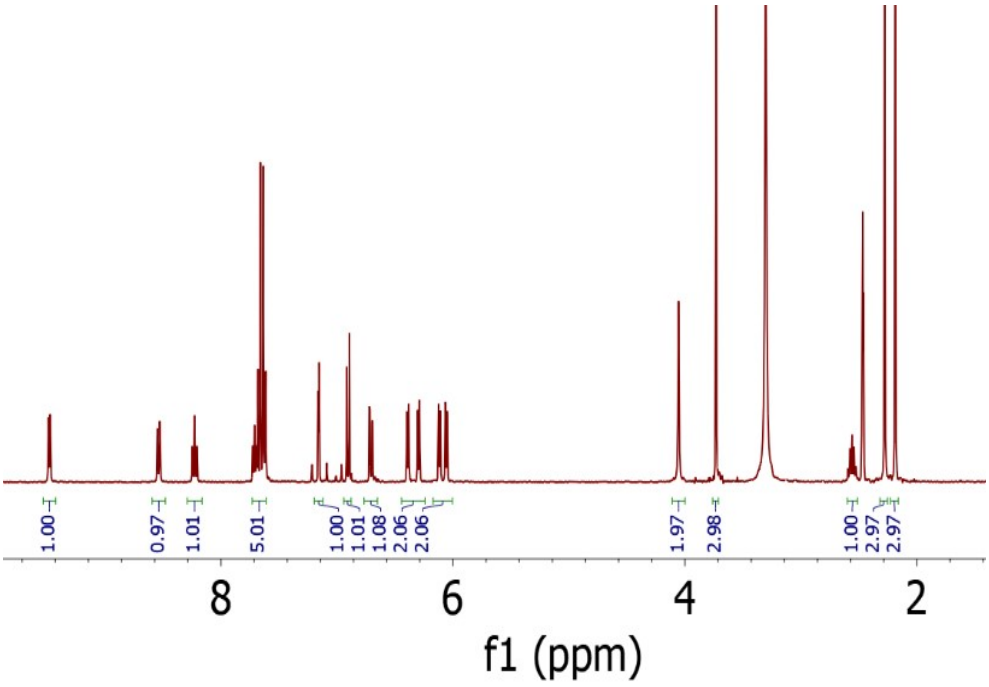

Figure S19. ^{1}H NMR spectrum of complex **2** in DMSO-d_6.

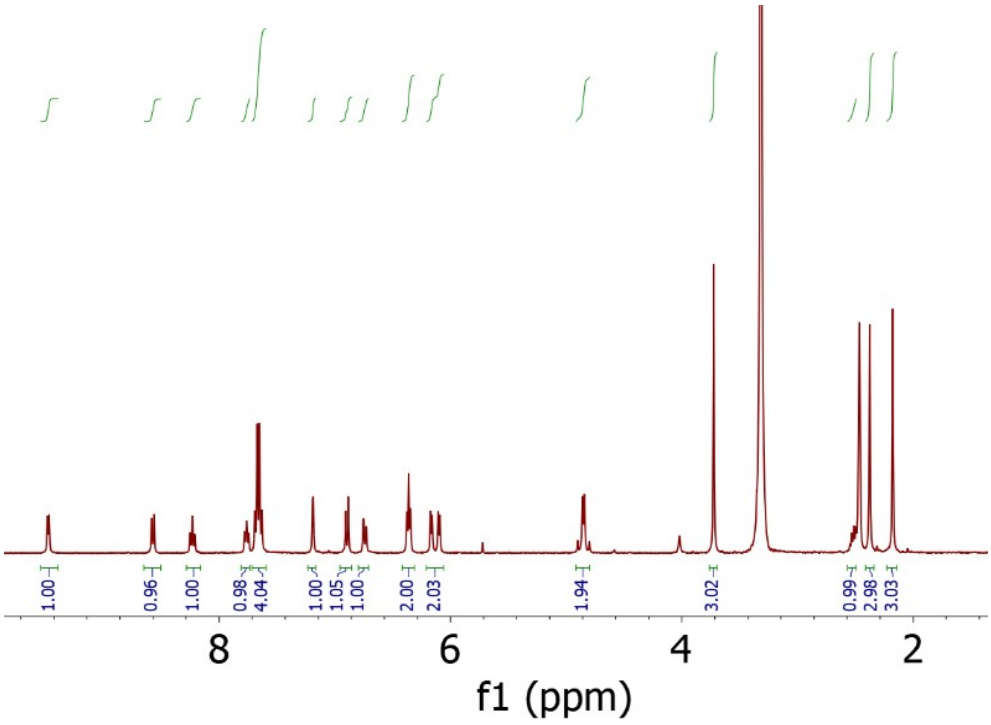

Figure S20. ^{1}H NMR spectrum of complex **3** in DMSO-d_6.

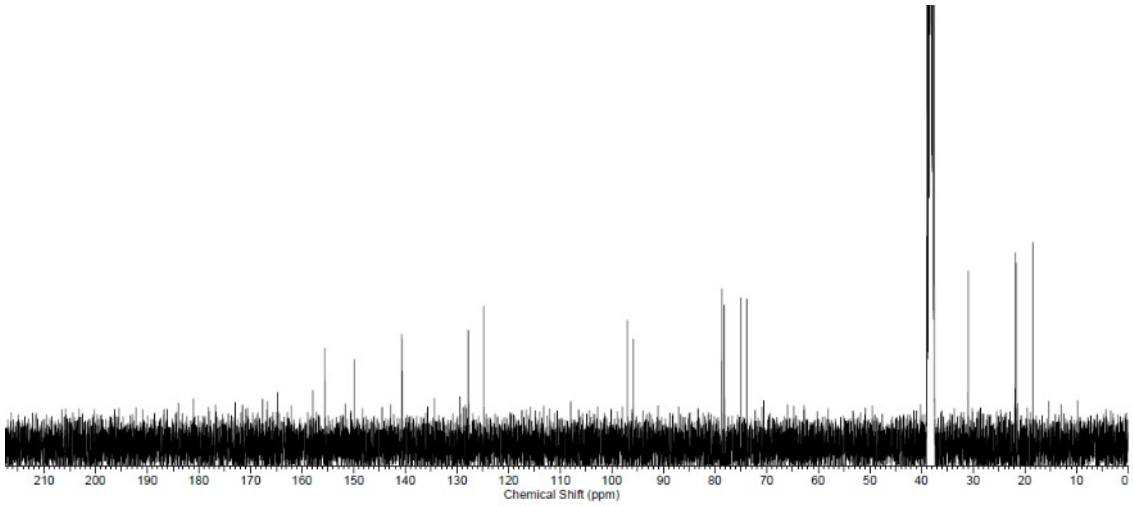

Figure S21. ^{13}C NMR spectrum of complex **1** in DMSO-d_6.

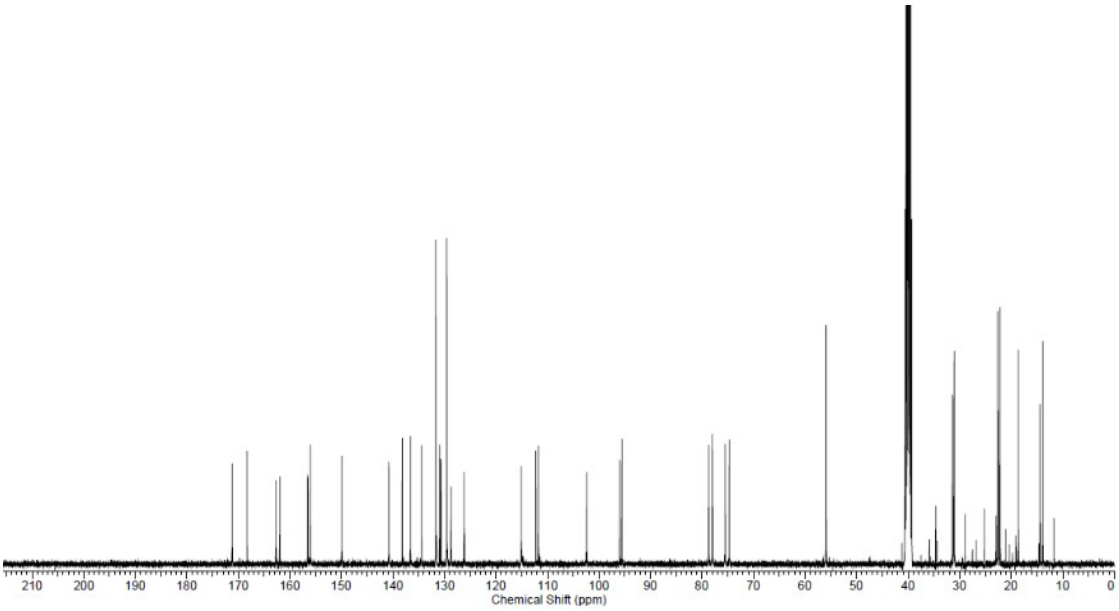

Figure S22. ^{13}C NMR spectrum of complex **2** in DMSO-d_6.

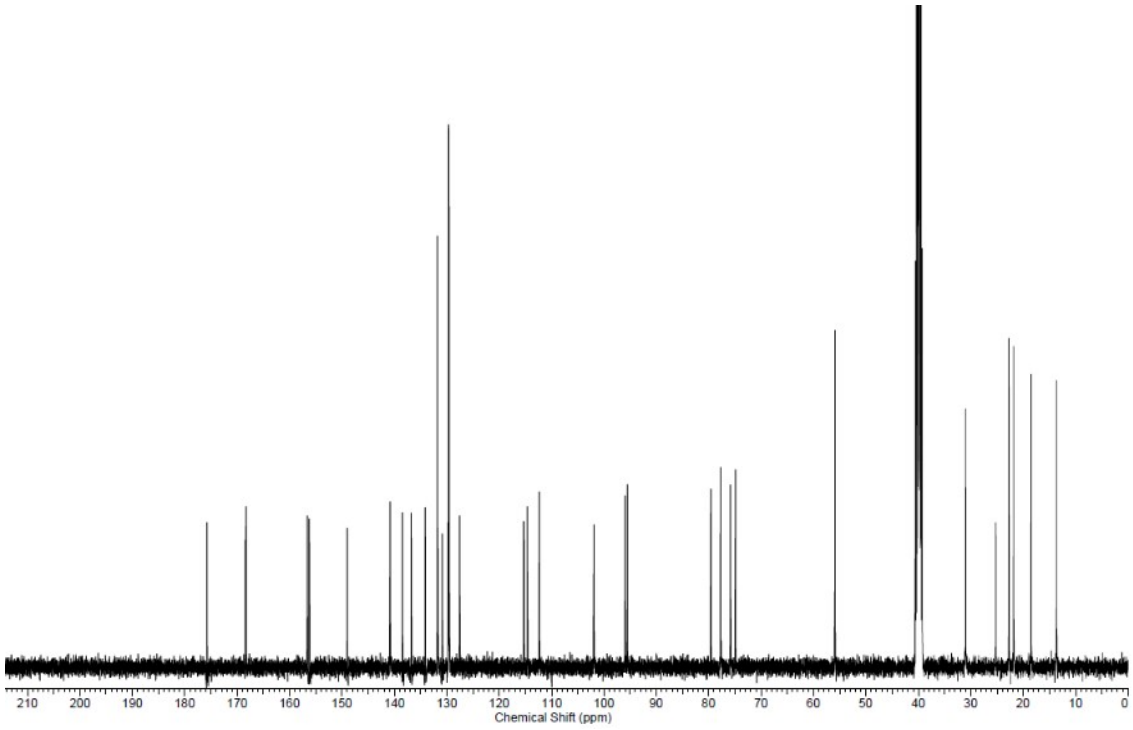

Figure S23. ^{13}C NMR spectrum of complex **3** in DMSO-d_6.

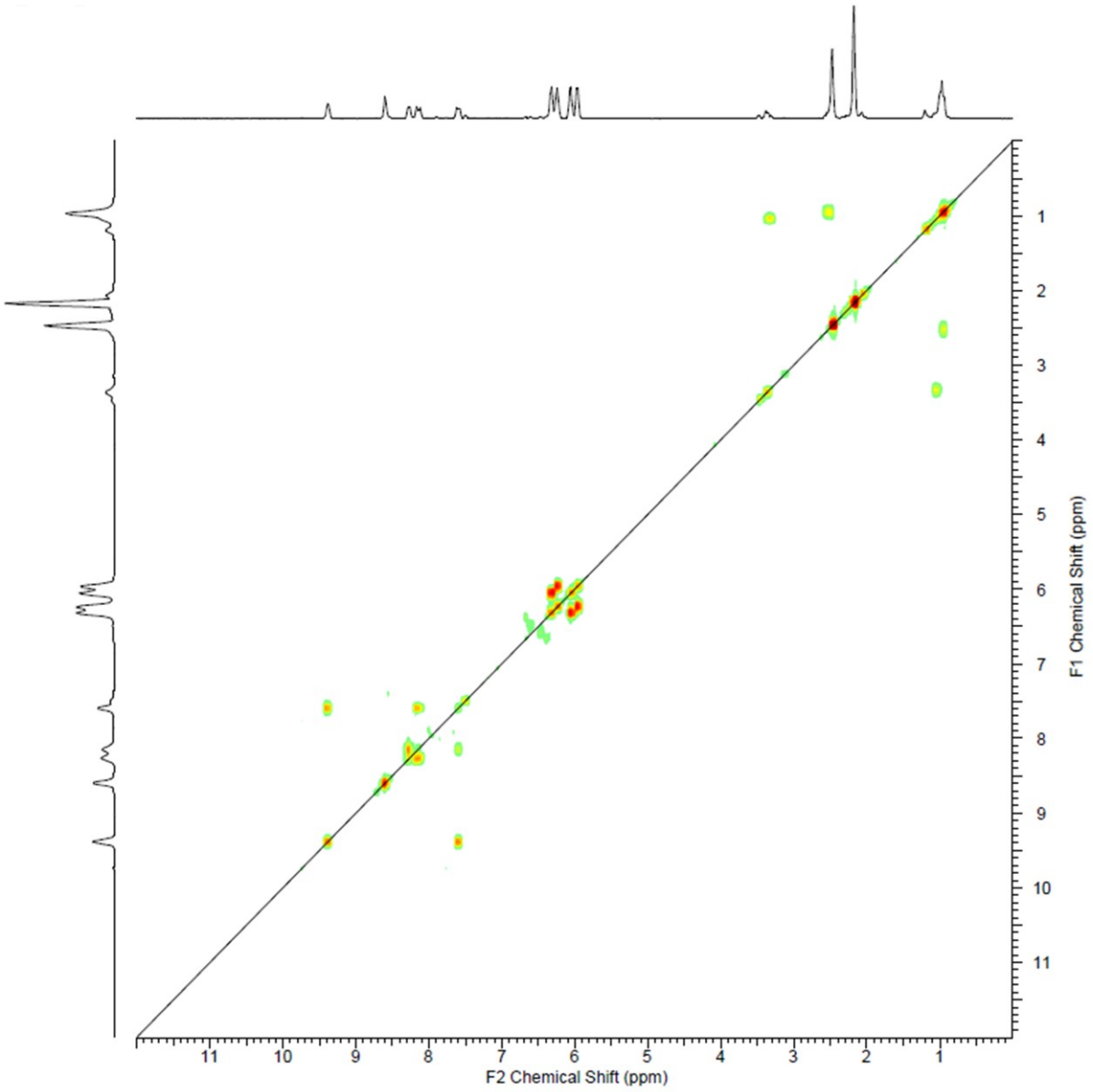

Figure S24. $^{1}H–^{1}H$ COSY spectrum of complex **1** (dissolved in DMSO-d_6).

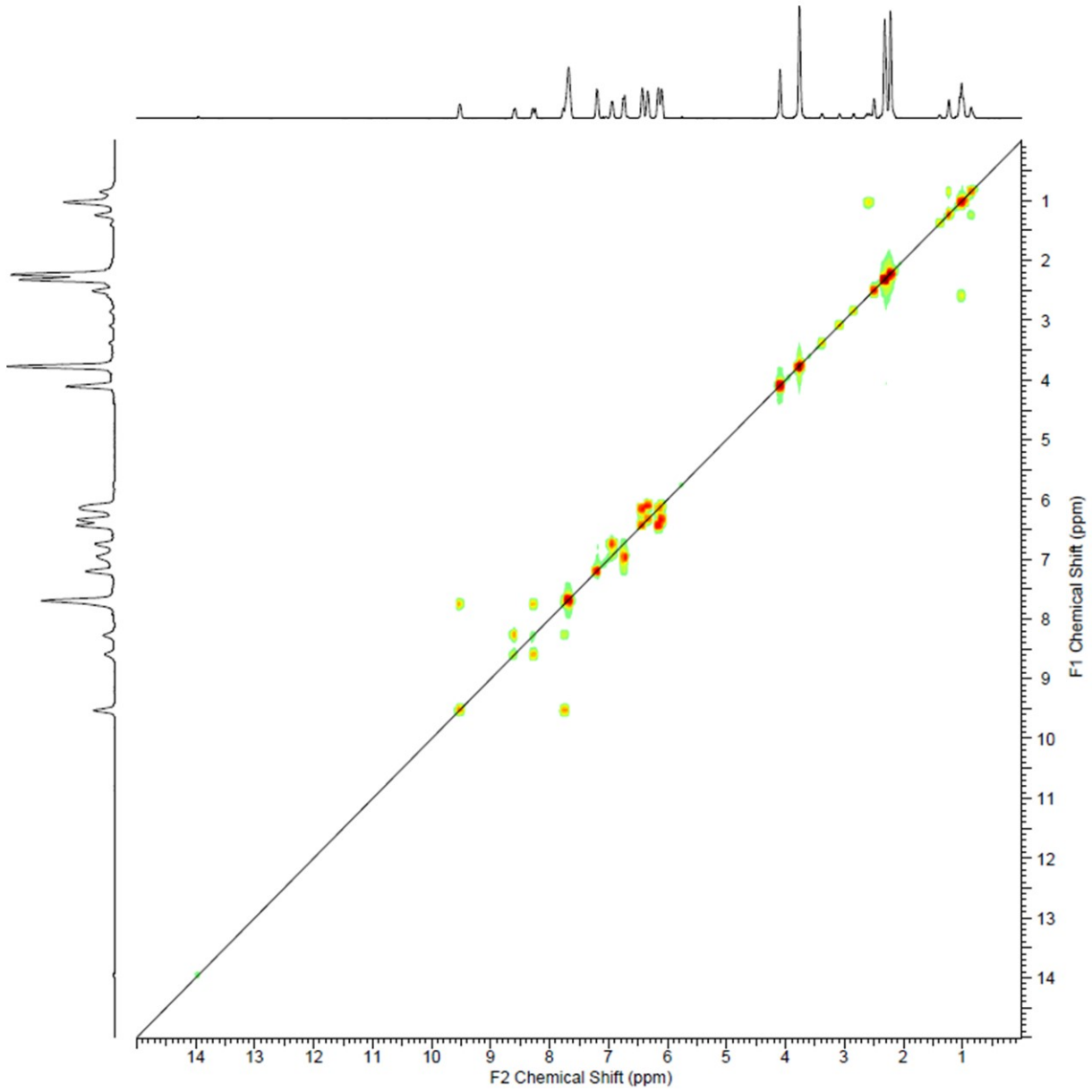

Figure S25. $^{1}H–^{1}H$ COSY spectrum of complex **2** (dissolved in DMSO-d_6).

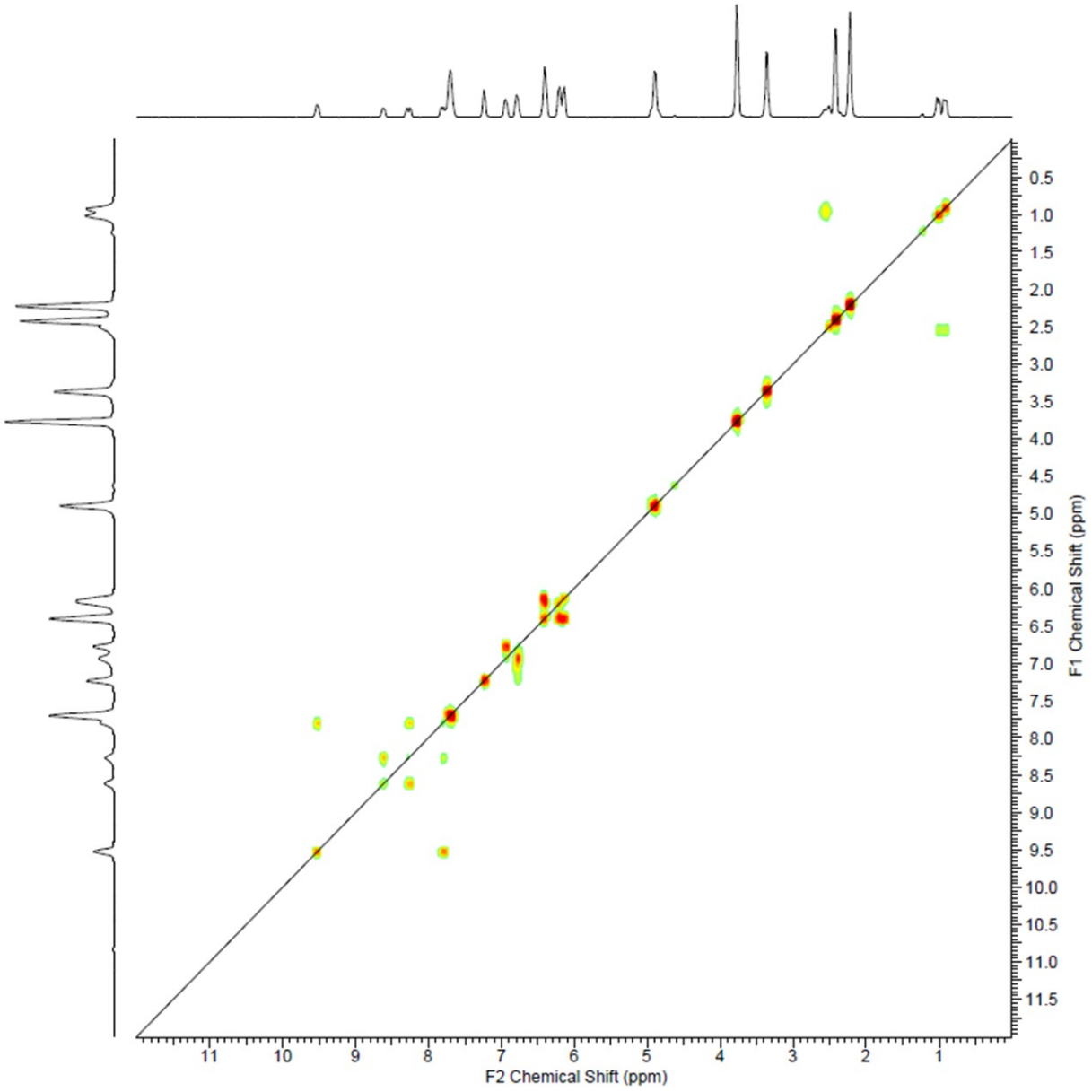

Figure S26. $^{1}H–^{1}H$ COSY spectrum of complex **3** (dissolved in DMSO-d_6).

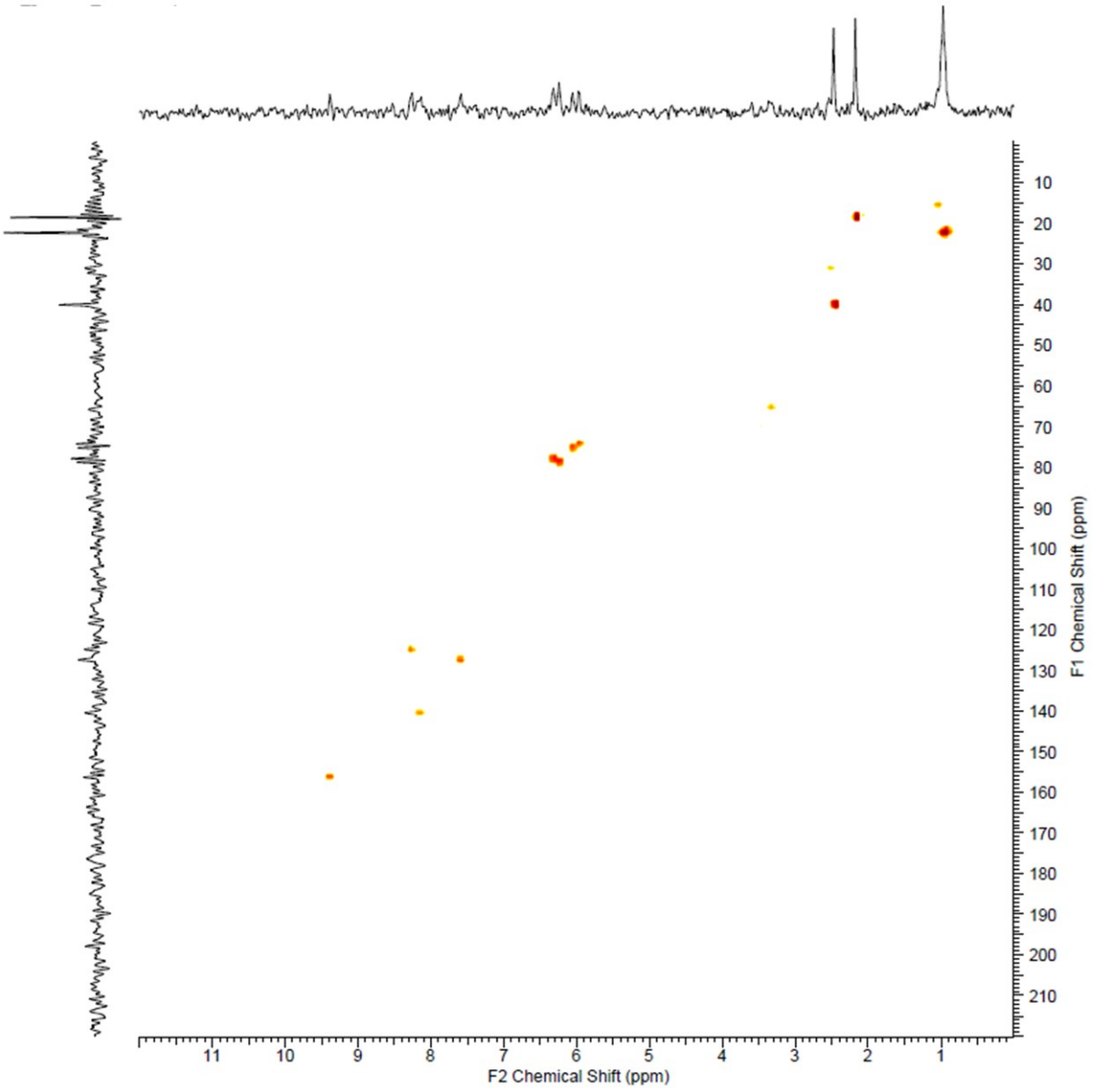

Figure S27. $^{1}H–^{13}C$ HMQC spectrum of complex **1** (dissolved in DMSO-d_6).

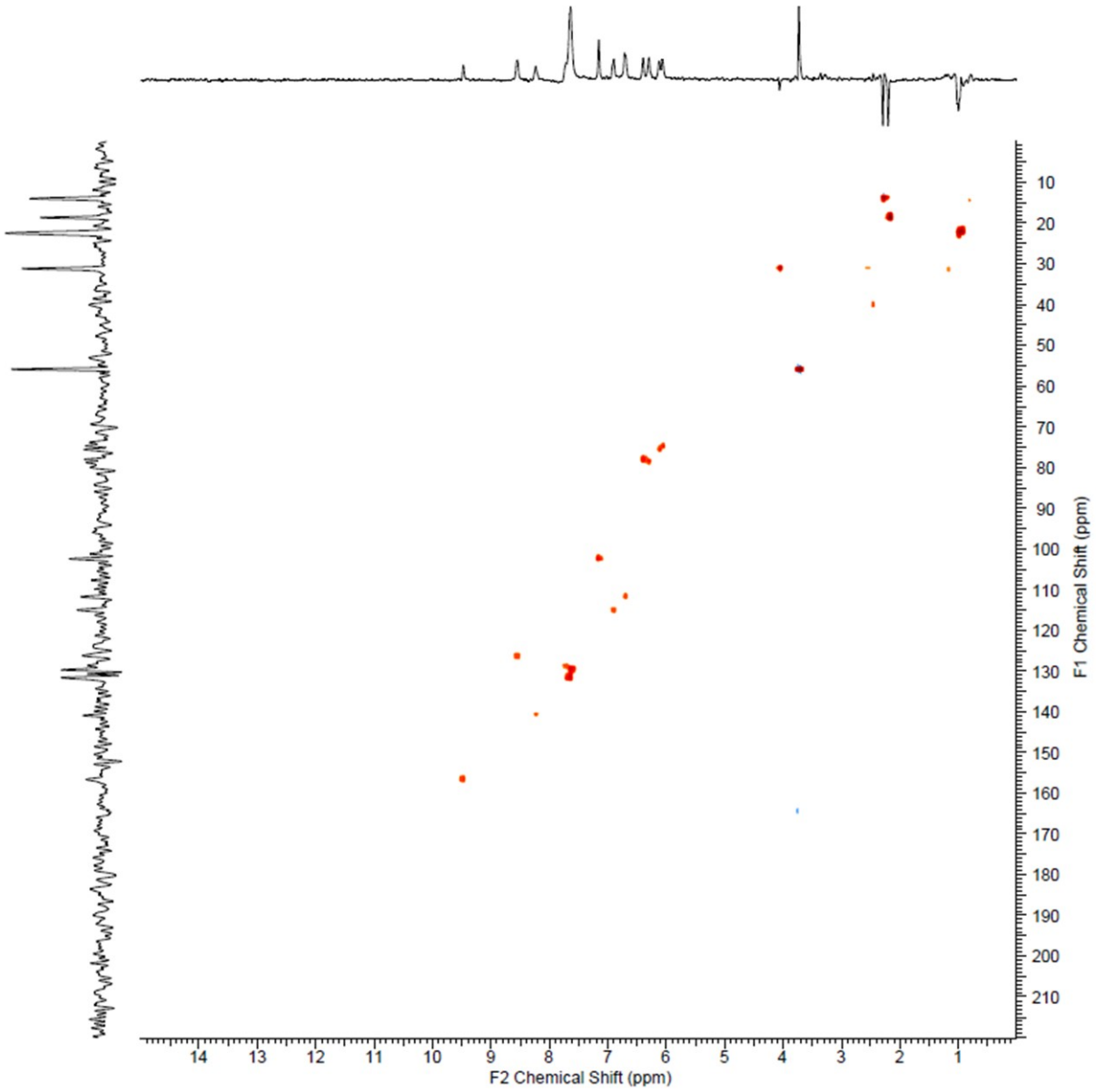

Figure S28. $^{1}H–^{13}C$ HMQC spectrum of complex **2** (dissolved in DMSO-d_6).

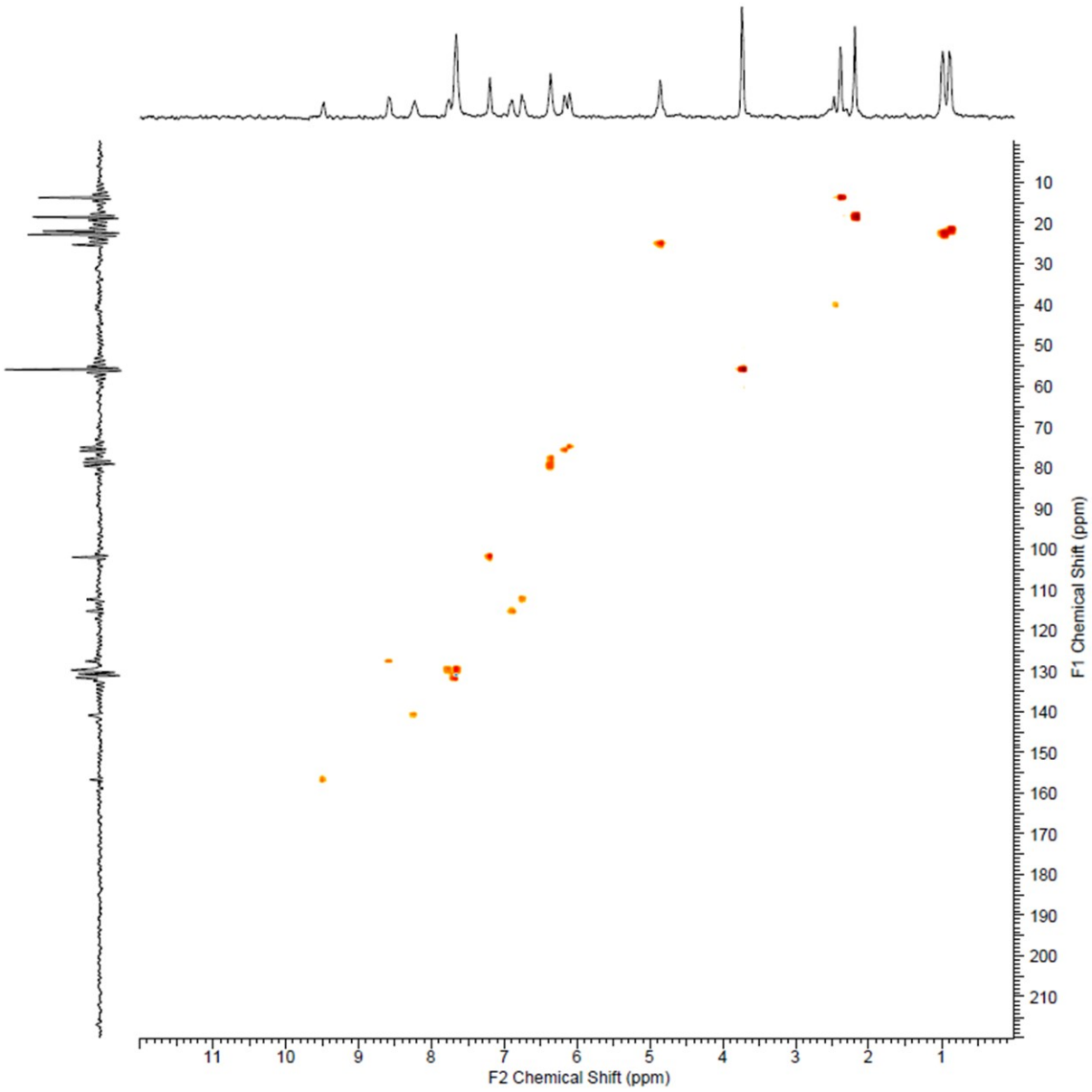

Figure S29. $^{1}H–^{13}C$ HMQC spectrum of complex **3** (dissolved in DMSO-d_6).

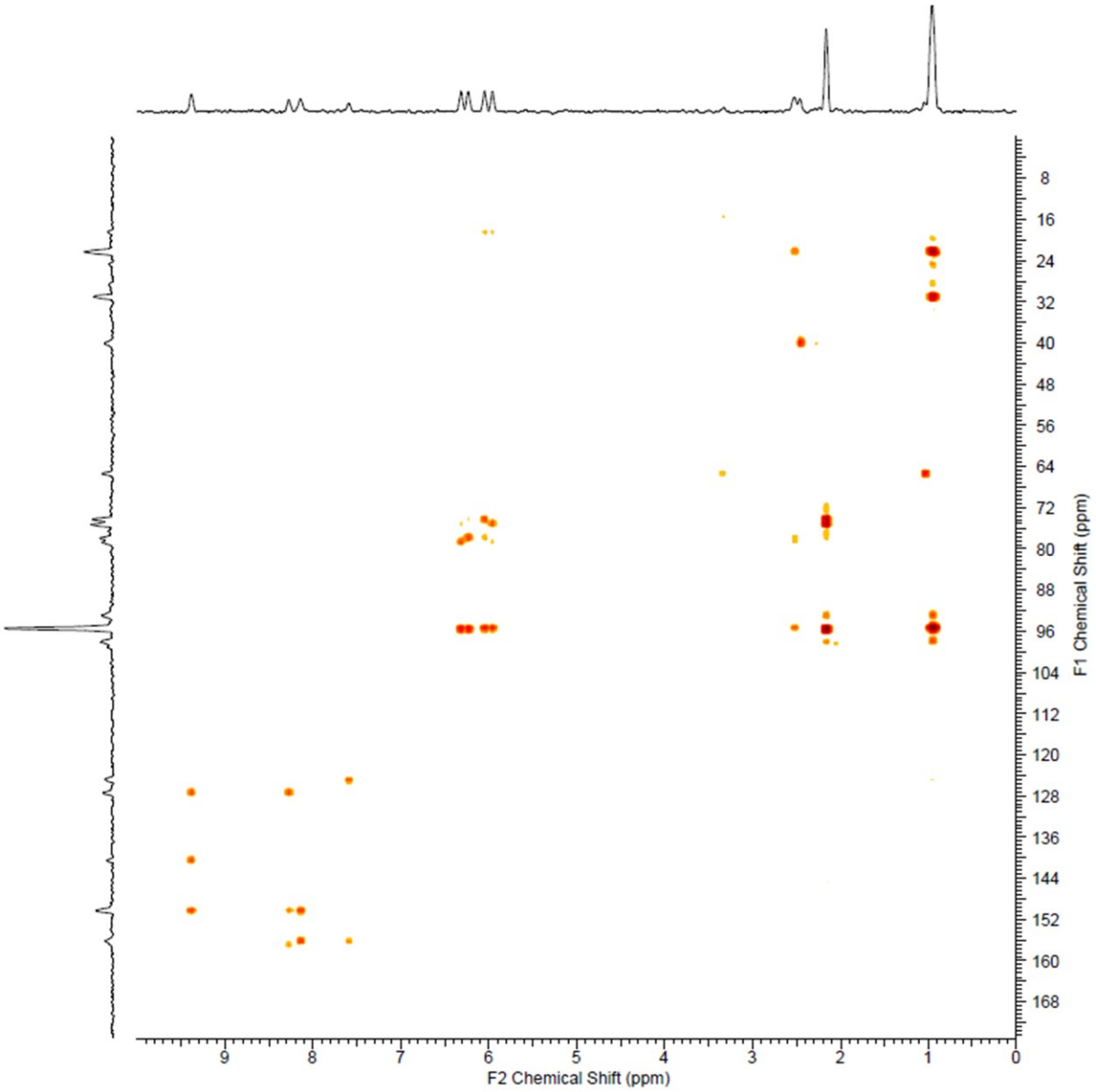

Figure S30. $^{1}H–^{13}C$ HMBC spectrum of complex **1** (dissolved in DMSO-d_6).

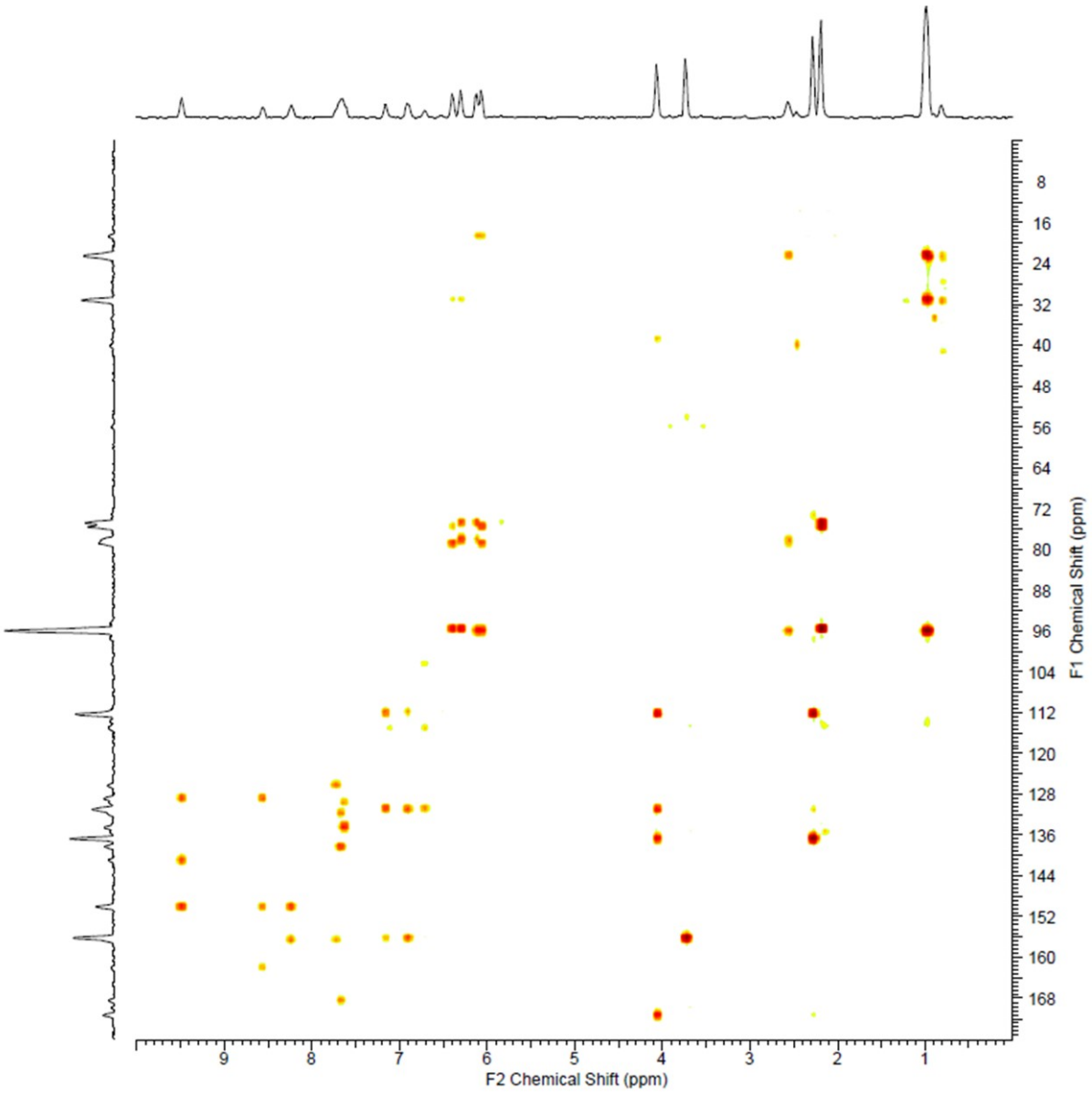

Figure S31. $^{1}H–^{13}C$ HMBC spectrum of complex **2** (dissolved in DMSO-d_6).

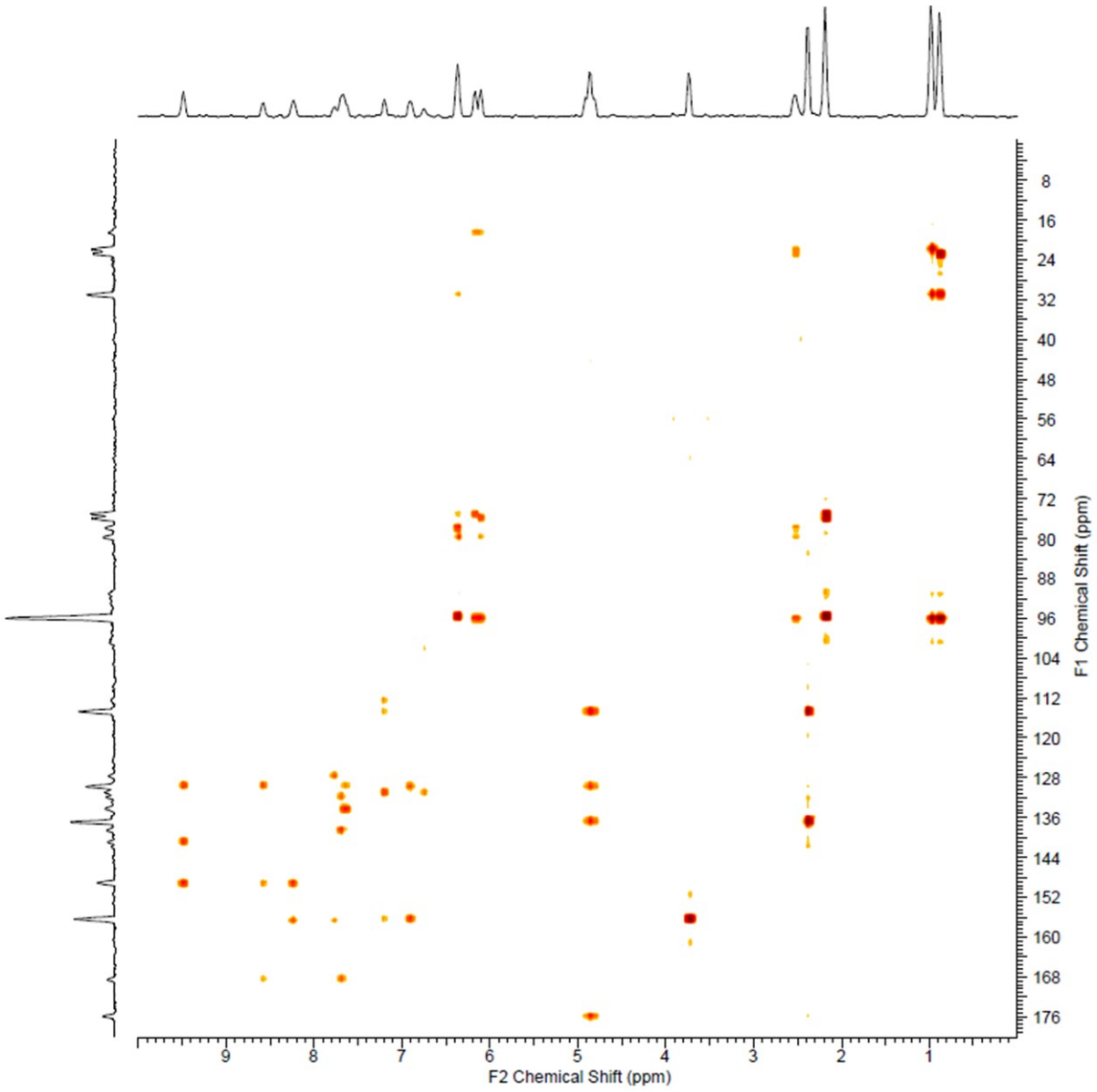

Figure S32. $^{1}H–^{13}C$ HMBC spectrum of complex **3** (dissolved in DMSO-d_6).

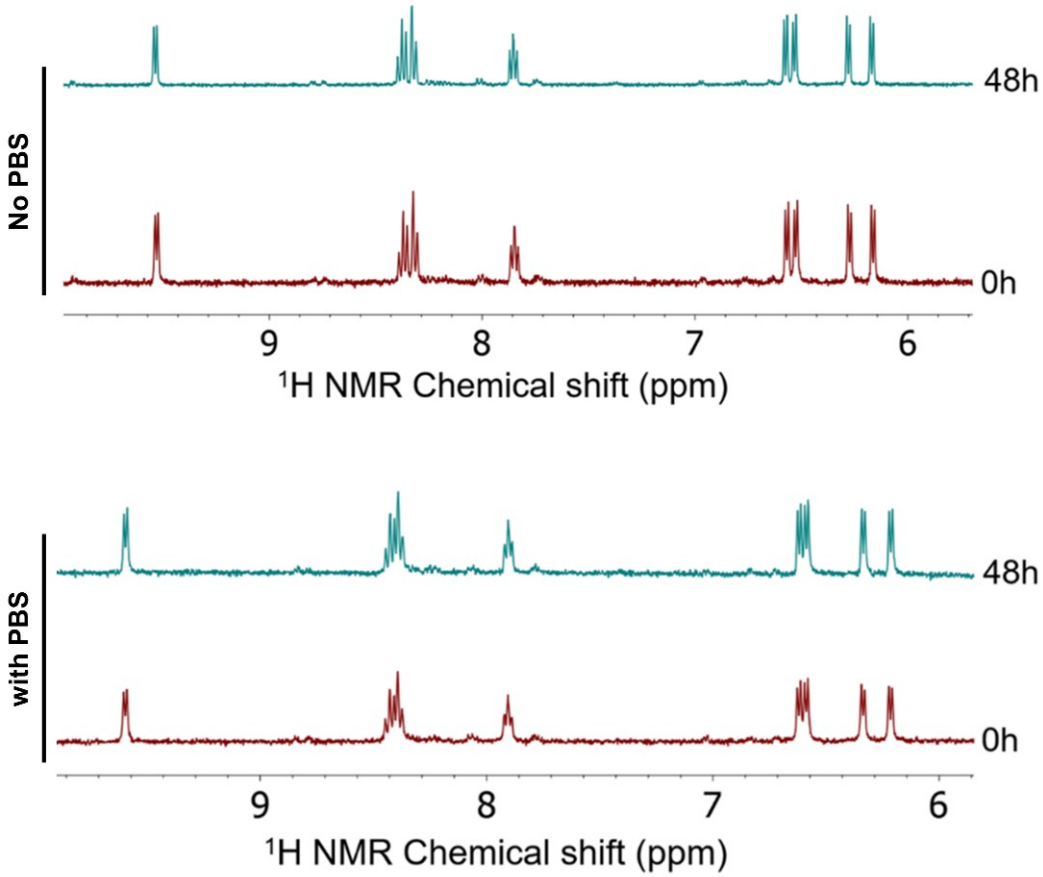

Figure S33. ^{1}H NMR studies of complex **1** in 40% DMSO-d_6/60% D_2O (*top*) and in 40% DMSO-d_7/60% PBS in D_2O (pH 7.4; *bottom*), as observed at different time points (0 h or 48 h).

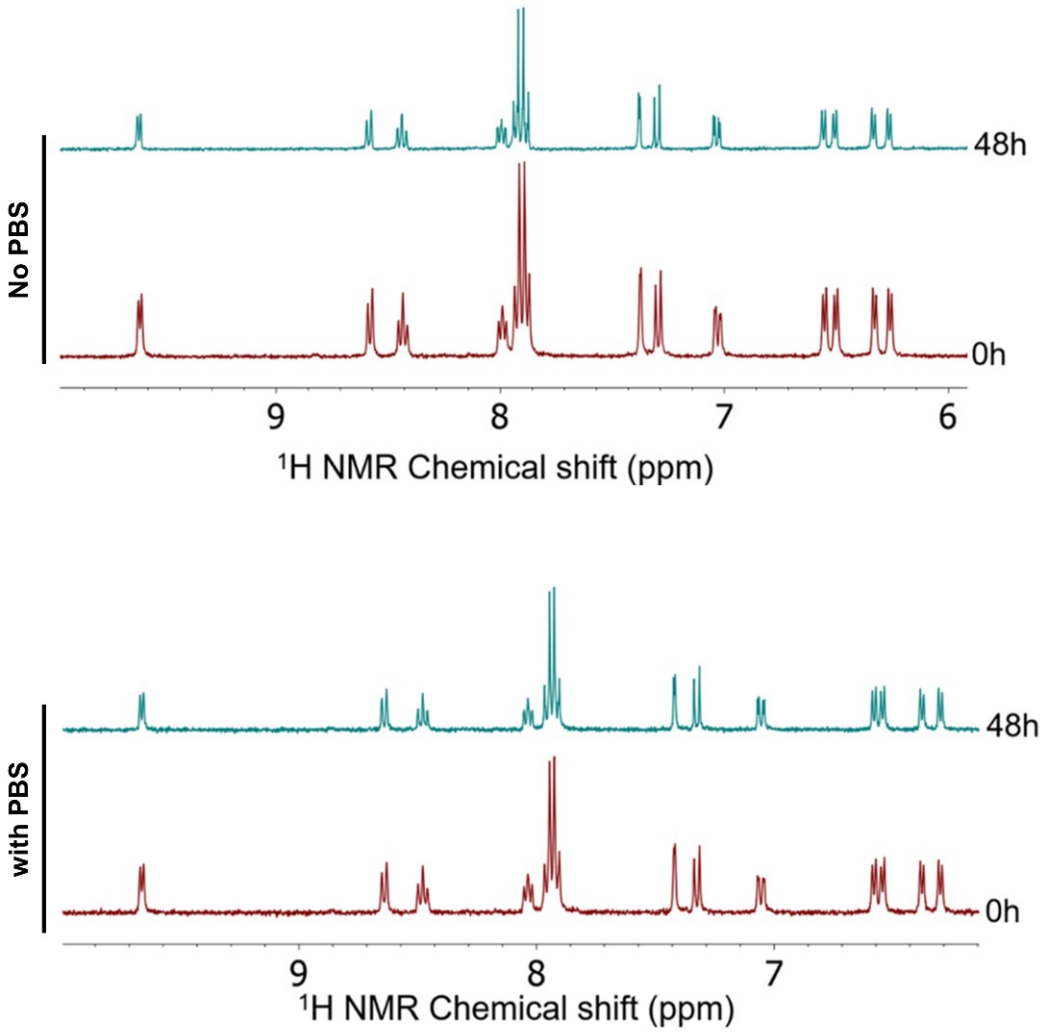

Figure S34. ^{1}H NMR studies of complex **2** in 40% DMSO-d_6/60% D_2O (*top*) and in 40% DMSO-d_7/60% PBS in D_2O (pH 7.4; *bottom*), as observed at different time points (0 h or 48 h).

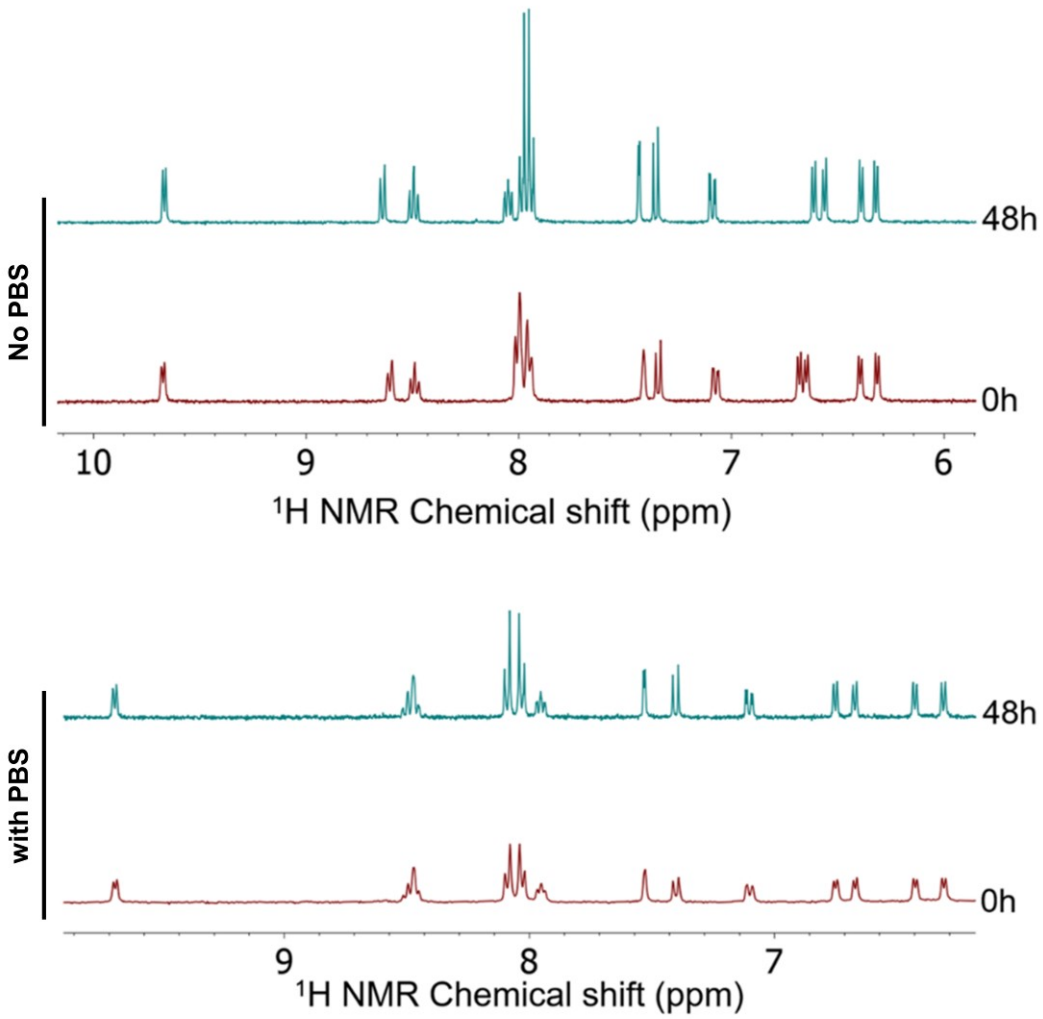

Figure S35. ^{1}H NMR studies of complex **3** in 40% DMSO-d_6/60% D_2O (*top*) and in 40% DMSO-d_7/60% PBS in D_2O (pH 7.4; *bottom*), as observed at different time points (0 h or 48 h).

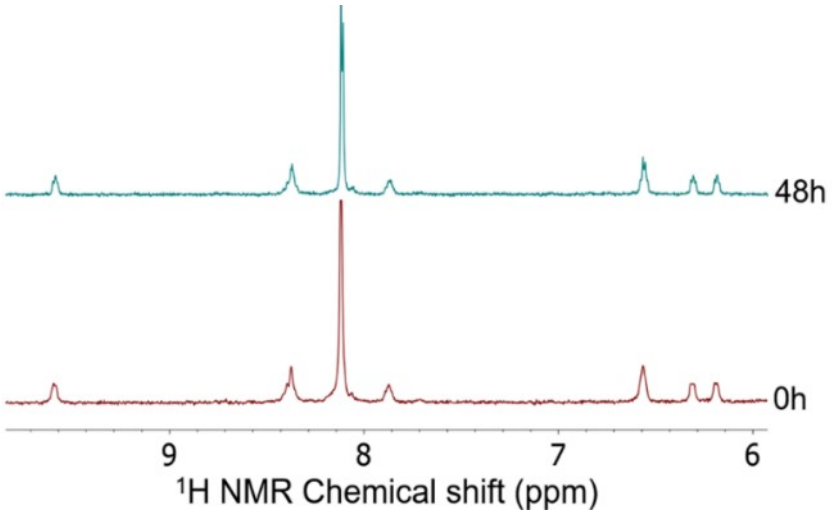

Figure S36. ^{1}H NMR studies of complex **1** in 40% DMF-d_7/60% PBS in D_2O (pH 7.4), as observed at different time points (0 h or 48 h).

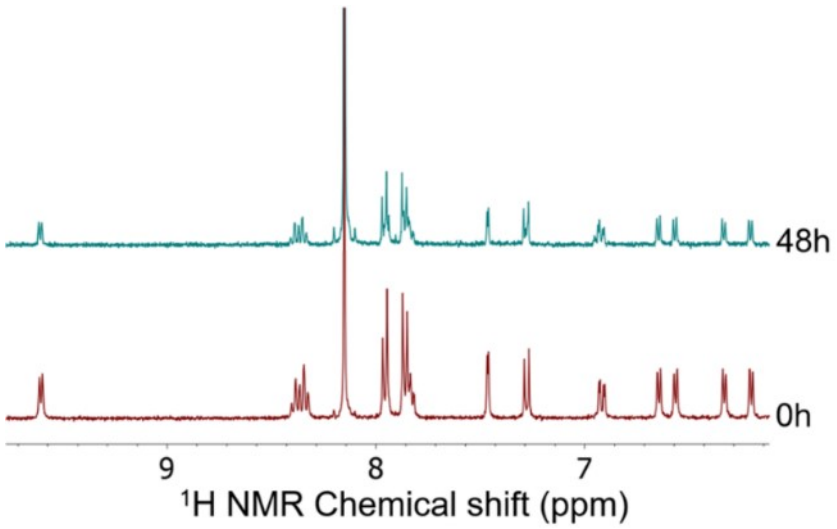

Figure S37. ^{1}H NMR studies of complex **2** in 40% DMF-d_7/60% PBS in D_2O (pH 7.4), as observed at different time points (0 h or 48 h).

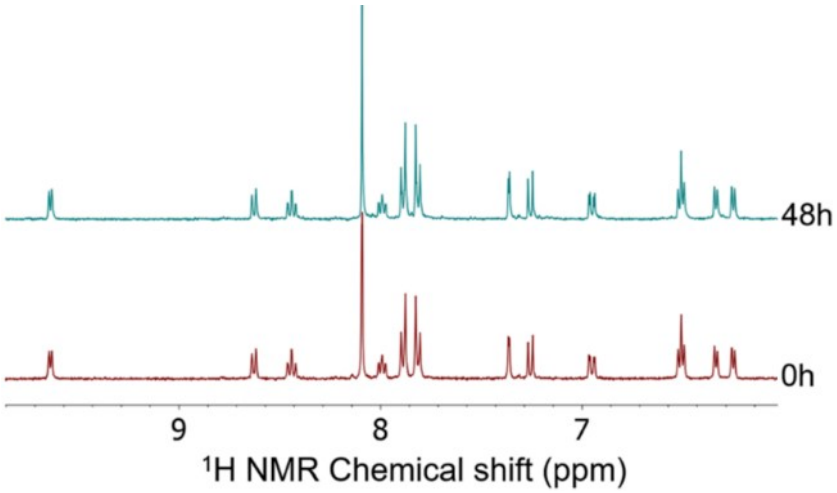

Figure S38. ^{1}H NMR studies of complex **3** in 40% DMF-d_7/60% PBS in D_2O (pH 7.4), as observed at different time points (0 h or 48 h).

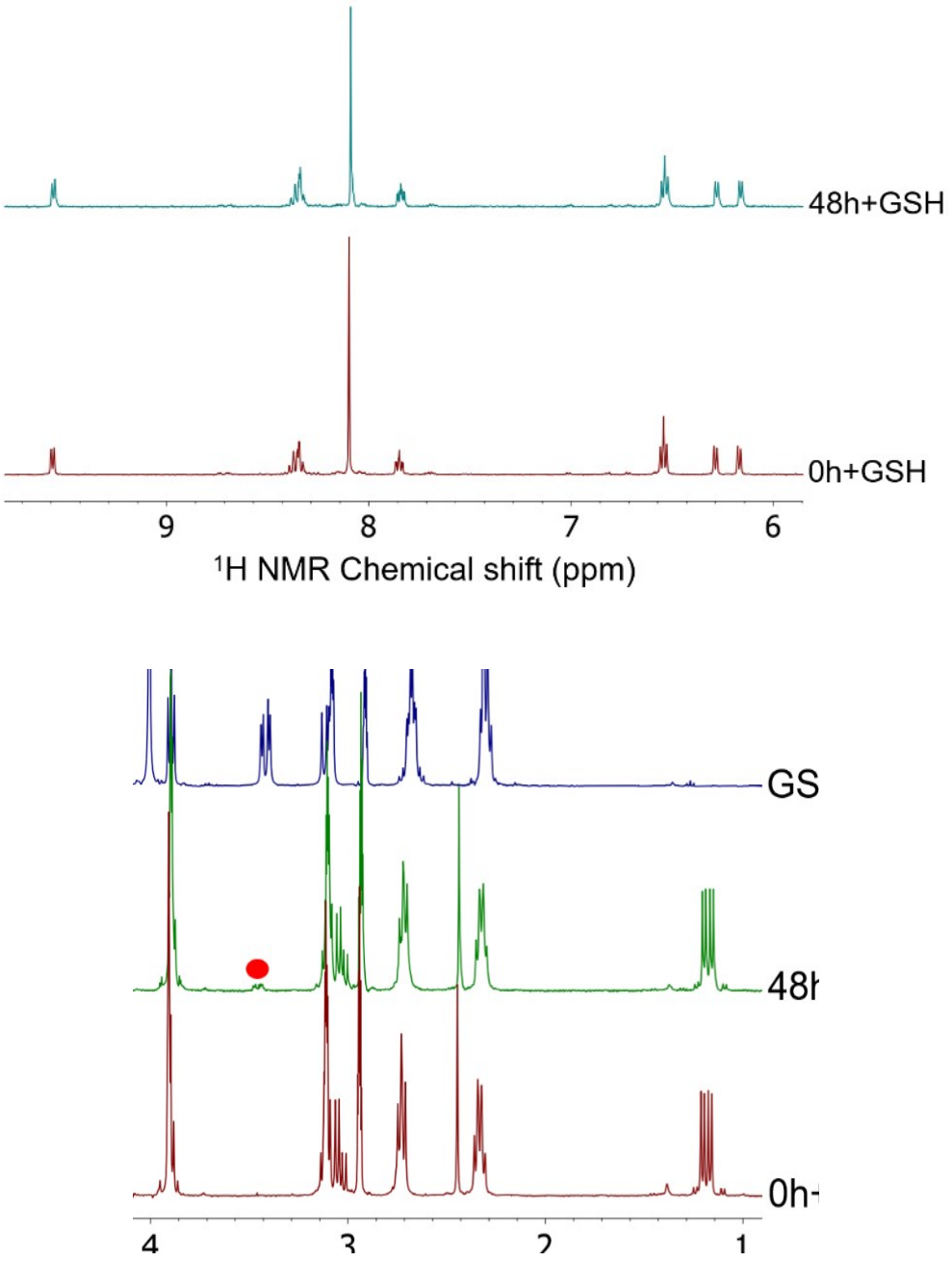

Figure S39. ^{1}H NMR studies of complex **1** in 40% DMF-d_7/60% PBS in D_2O (pH 7.4) with 5 molar equivalents of GSH, as observed at different time points (0 h or 48 h). The spectrum of free glutathione disulfide (GSSG) is given for comparative purposes. Red sphere = Cys-β CH_2 of GSSG.

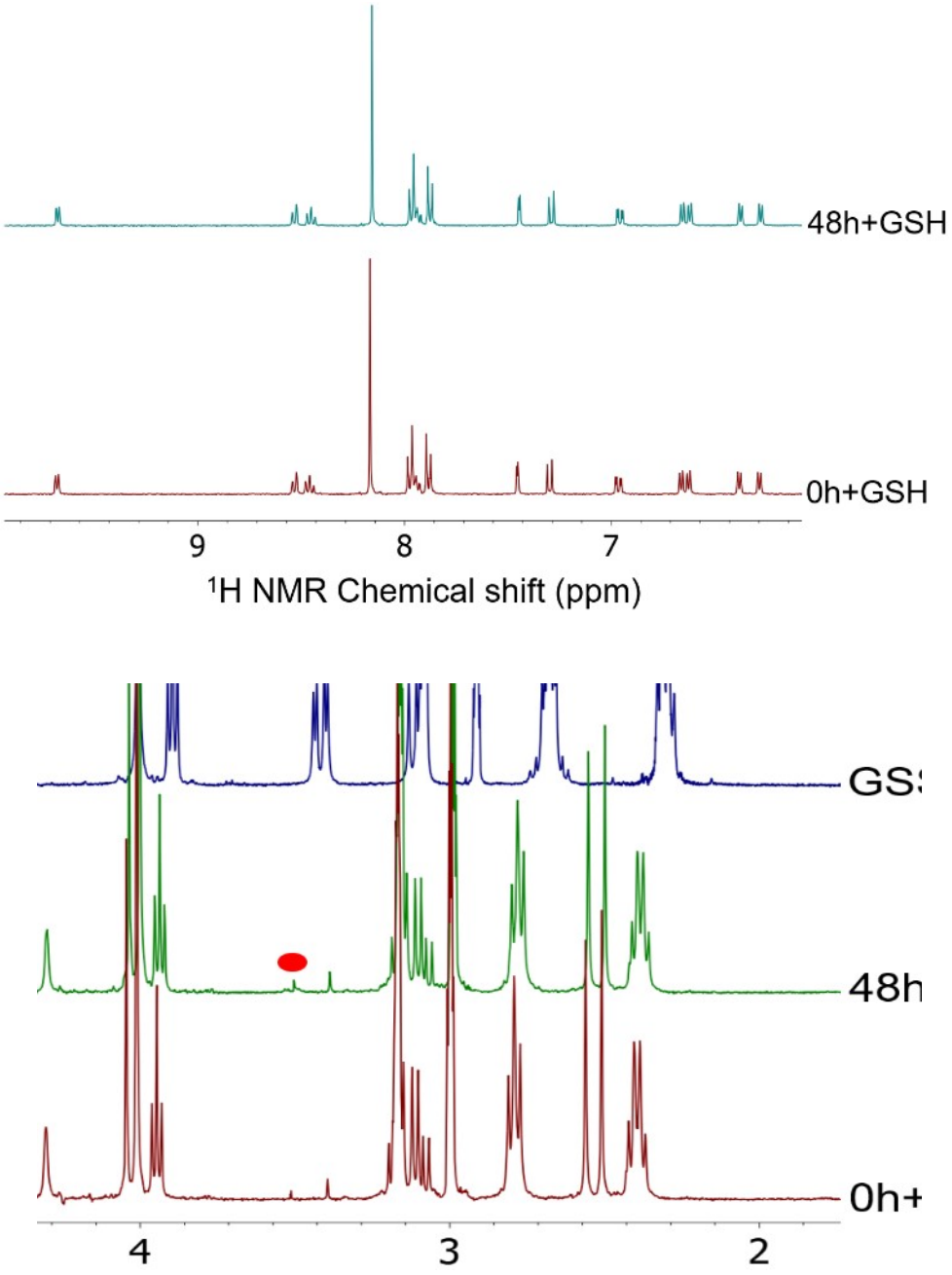

Figure S40. ^{1}H NMR studies of complex **2** in 40% DMF-d_7/60% PBS in D_2O (pH 7.4) with 5 molar equivalents of GSH, as observed at different time points (0 h or 48 h). The spectrum of free glutathione disulfide (GSSG) is given for comparative purposes. Red sphere = Cys-β CH_2 of GSSG.

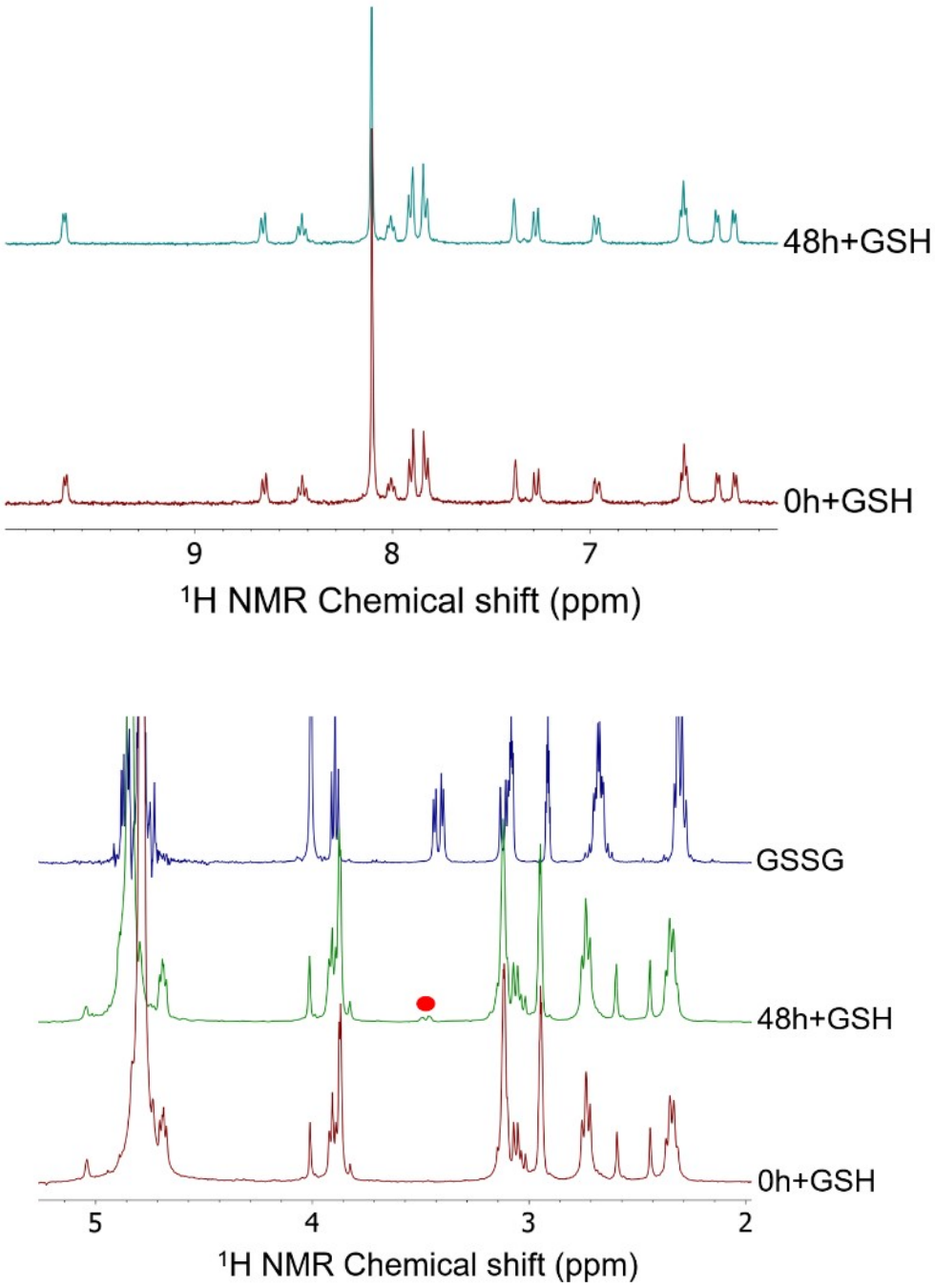

Figure S41. ^{1}H NMR studies of complex **3** in 40% DMF-d_7/60% PBS in D_2O (pH 7.4) with 5 molar equivalents of GSH, as observed at different time points (0 h or 48 h). The spectrum of free glutathione disulfide (GSSG) is given for comparative purposes. Red sphere = Cys-β CH_2 of GSSG.

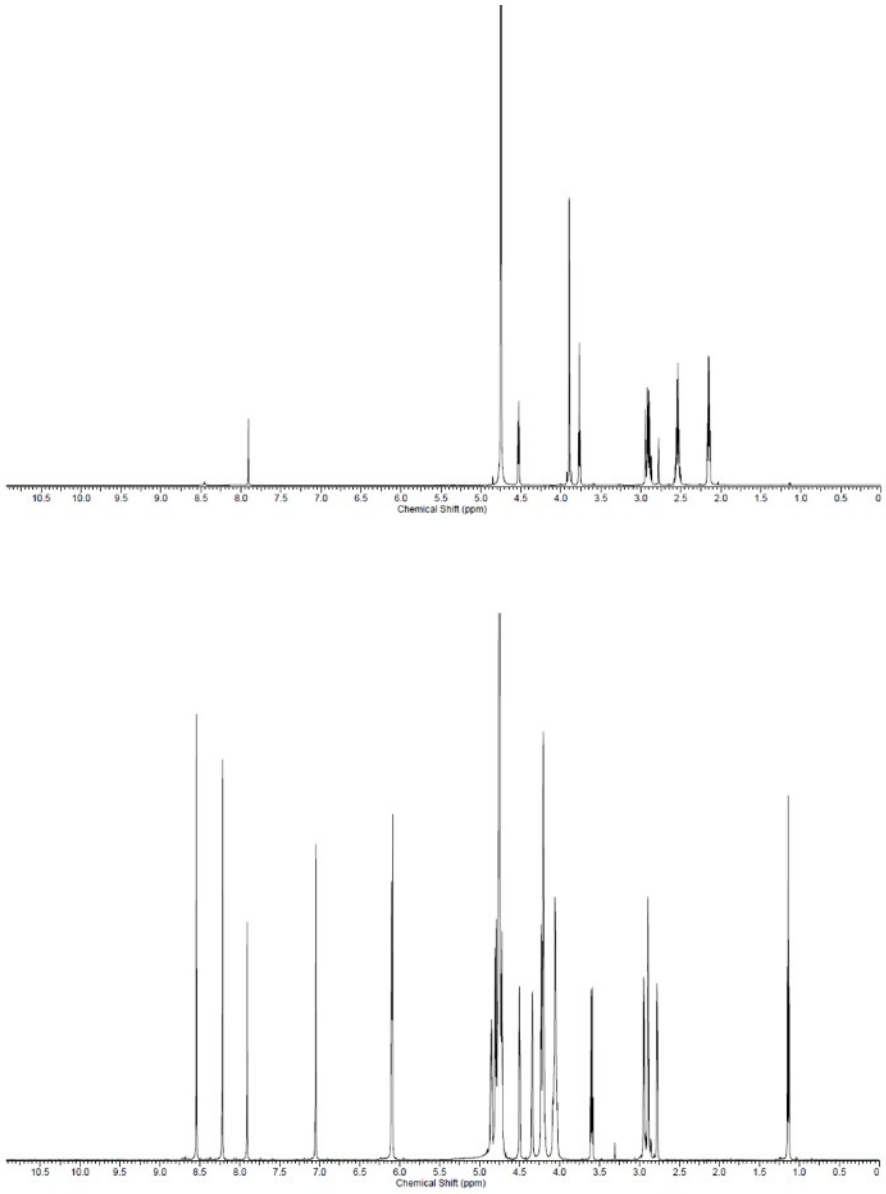

Figure S42. ^{1}H NMR control studies of free reduced glutathione (GSH; *top*) and nicotinamide adenine dinucleotide, reduced (NADH; *bottom*) in 40% DMF-d_7/60% PBS in D_2O (pH 7.4) after 48 h of standing at r.t.

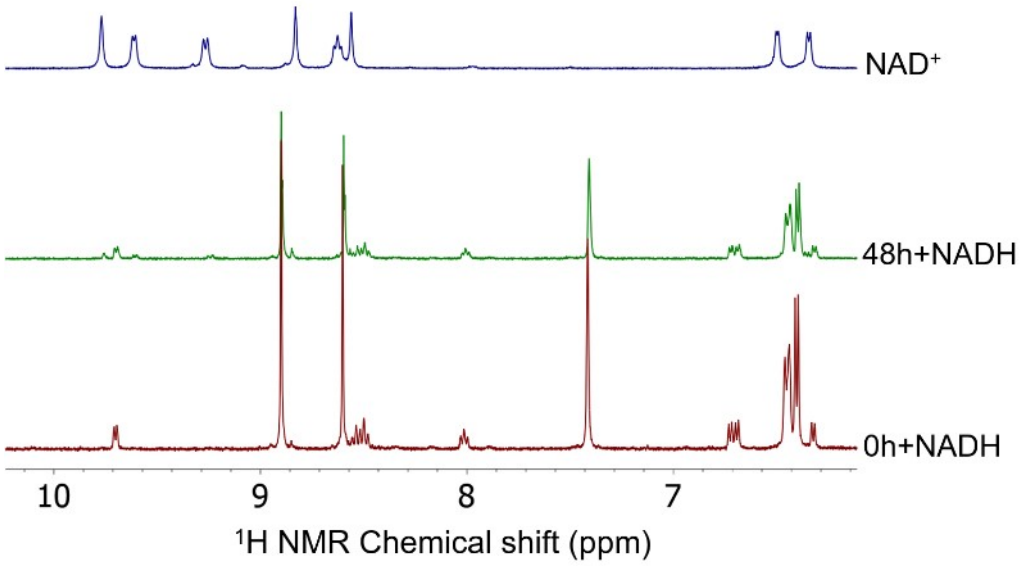

Figure S43. ^{1}H NMR studies of complex **1** in 40% DMSO-d_6/60% PBS in D_2O (pH 7.4) with 5 molar equivalents of NADH, as observed at different time points (0 h or 48 h). The spectrum of free NAD^+ is given for comparative purposes.

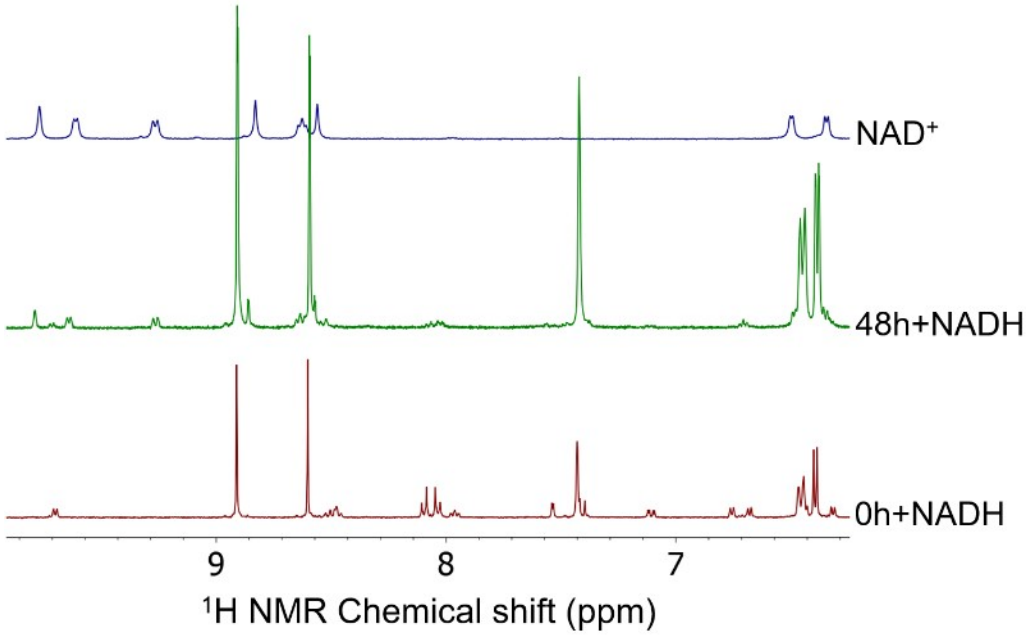

Figure S44. ^{1}H NMR studies of complex **2** in 40% DMSO-d_6/60% PBS in D_2O (pH 7.4) with 5 molar equivalents of NADH, as observed at different time points (0 h or 48 h). The spectrum of free NAD^+ is given for comparative purposes.

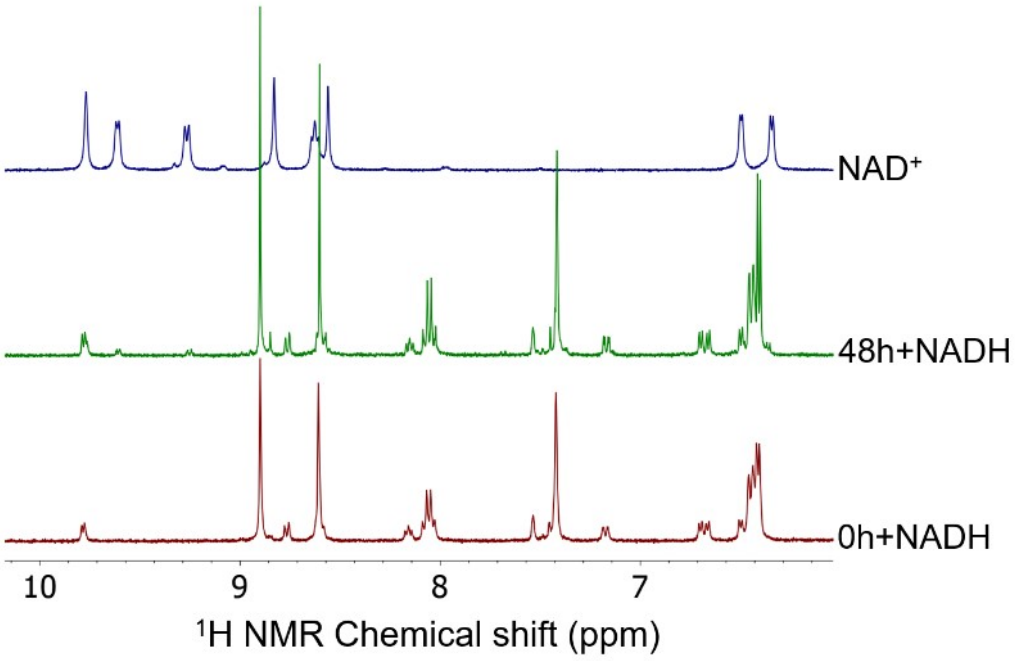

Figure S45. ^{1}H NMR studies of complex **3** in 40% DMSO-d_6/60% PBS in D_2O (pH 7.4) with 5 molar equivalents of NADH, as observed at different time points (0 h or 48 h). The spectrum of free NAD^+ is given for comparative purposes.

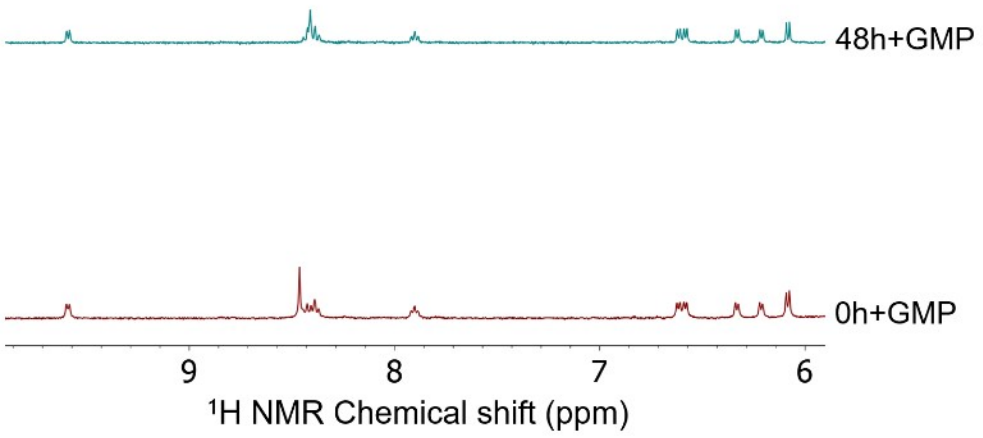

Figure S46. ^{1}H NMR studies of complex **1** in 40% DMSO-d_6/60% PBS in D_2O (pH 7.4) with 5 molar equivalents of GMP, as observed at different time points (0 h or 48 h).

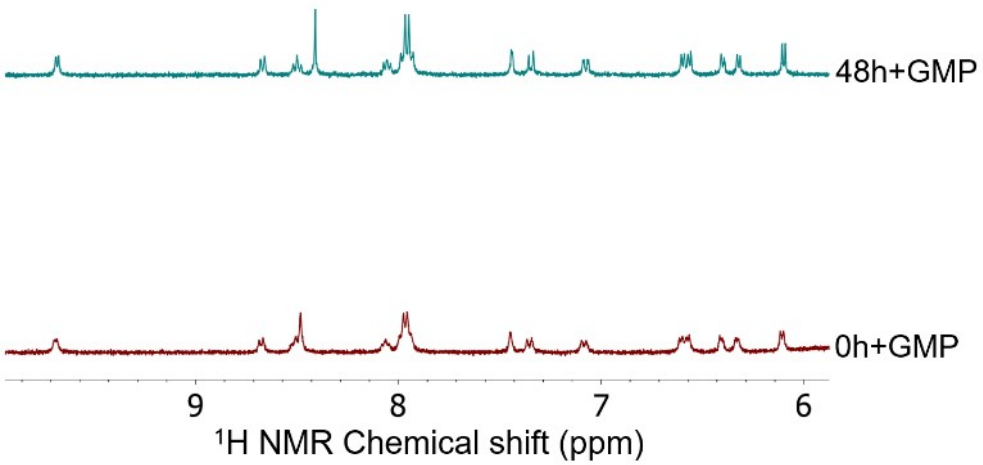

Figure S47. ^{1}H NMR studies of complex **3** in 40% DMSO-d_6/60% PBS in D_2O (pH 7.4) with 5 molar equivalents of GMP, as observed at different time points (0 h or 48 h).

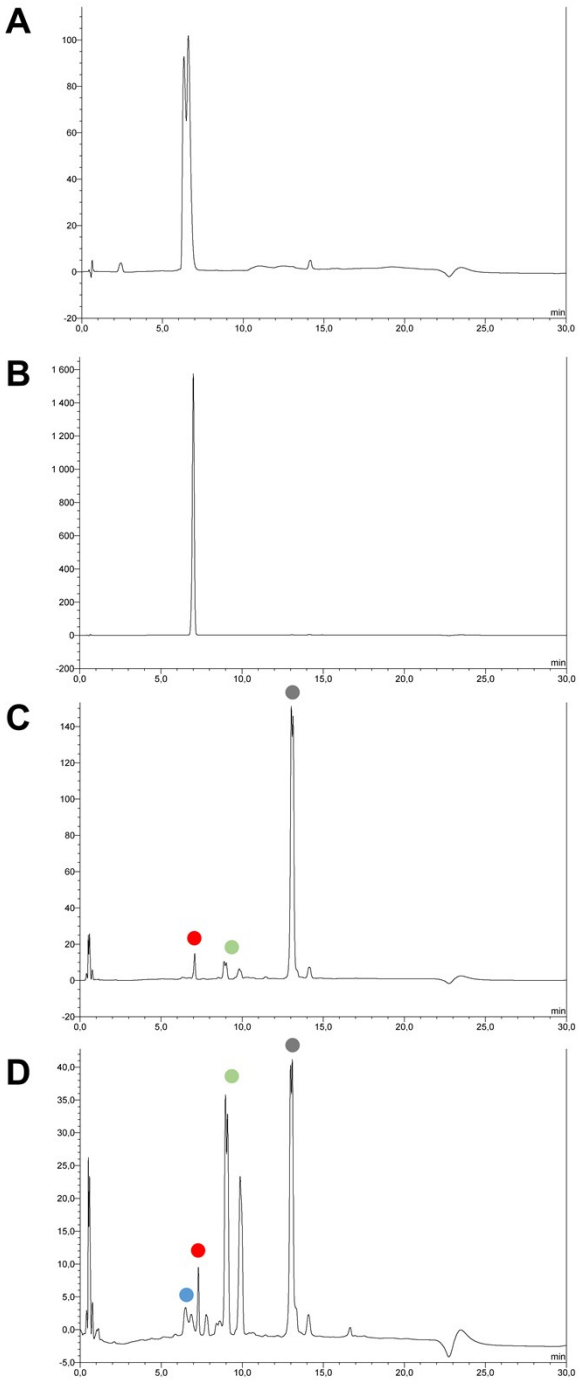

Figure S48. The results of RP-HPLC coupled with ESI+ mass spectrometry for **1** (***A***), indomethacin (***B***), and for the mixture of **2** with carboxypeptidase A from bovine pancreases (CAP A) at *t* = 0 h (***C***) and *t* = 24 f (***D***). Blue sphere - **1**; red sphere - indomethacin; green sphere - new Os-containing species (see Figure S50 below); grey sphere - **2**.

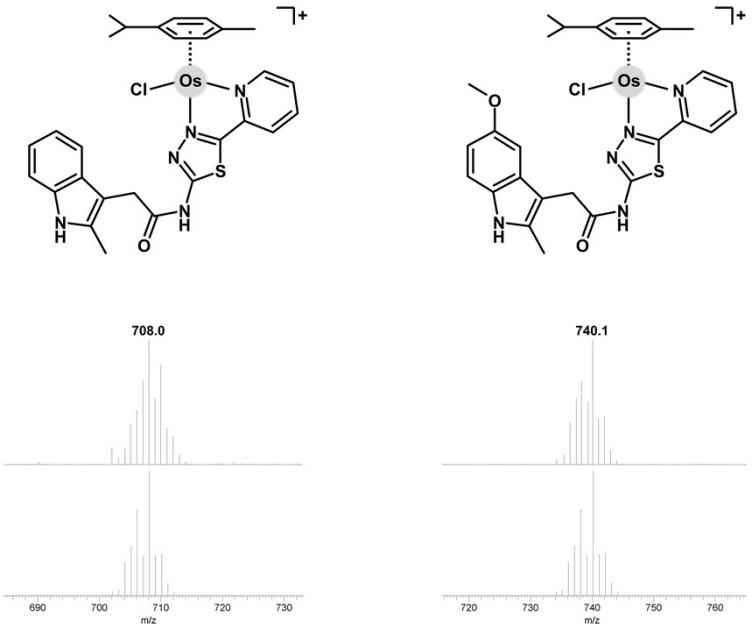

Figure S49. The Os-containing species, which formed (together with complex **1**) from the studied complex **2** under the RP-HPLC conditions in the presence of carboxypeptidase A from bovine pancreases (CAP A), given together with the ESI+ mass spectra (*top* - experimental; *bottom* - theoretical) proving their composition. These species were detected at t_R = 9.76 min (740.1 *m/z*) and 8.94 min (708.0 *m/z*) by HPLC.

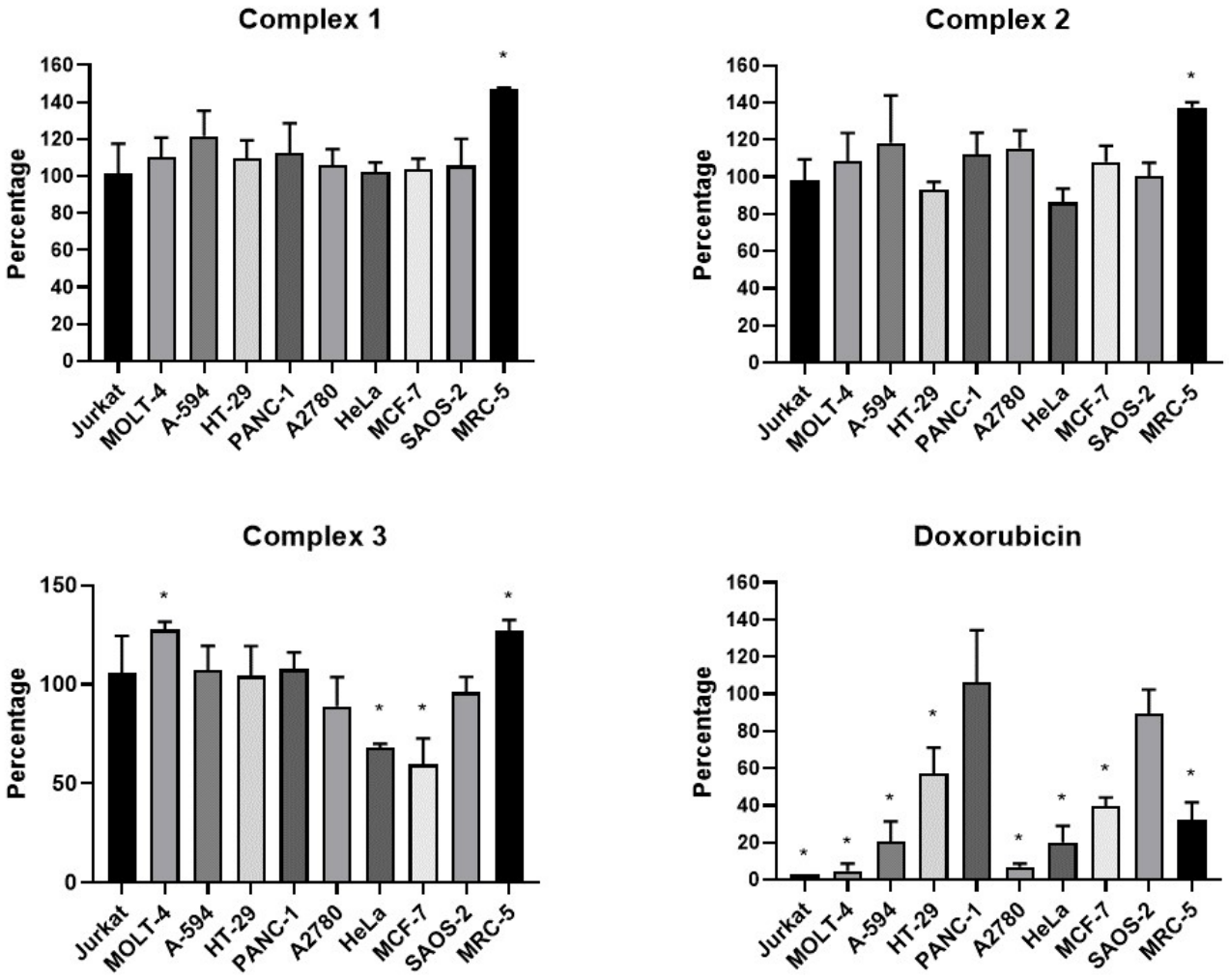

Figure S50. The *in vitro* cytotoxicity results for complexes **1–3** (applied at 10 μM concentration) and doxorubicin (applied at 1 μM concentration) against human Jurkat (acute T cell leukemia), MOLT-4 (acute lymphoblastic leukemia), A549 (lung carcinoma), HT-29 (colorectal adenocarcinoma), PANC-1 (pancreas epithelioid carcinoma), A2780 (ovarian carcinoma), HeLa (cervix adenocarcinoma), MCF-7 (breast adenocarcinoma), SAOS-2 (osteosarcoma) and MRC-5 (normal lung fibroblasts) cell lines (48 h exposure, WST-1 proliferation assay). Data are presented as the mean ± SD of percentage relative to untreated cells, arbitrary set to 100%. Significance was tested using One-sample T-test. * $p \leq 0.05$

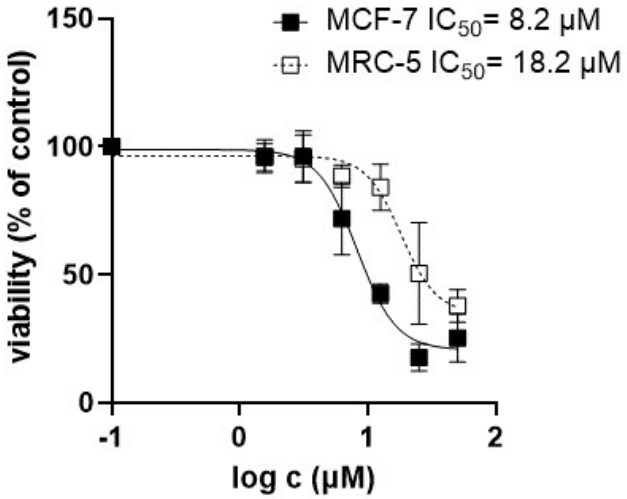

Figure S51. Dose response of the MCF-7 breast adenocarcinoma cells and MRC-5 normal lung fibroblasts to the treatment with complex **3**. Cell proliferation/viability was measured using the colorimetric WST-1 assay after 48 h of the treatment with **3**. Data are presented as the percentage relative to untreated cells, arbitrary set to 100%. The data points in the graph are the means ± SD of three independent experiments.

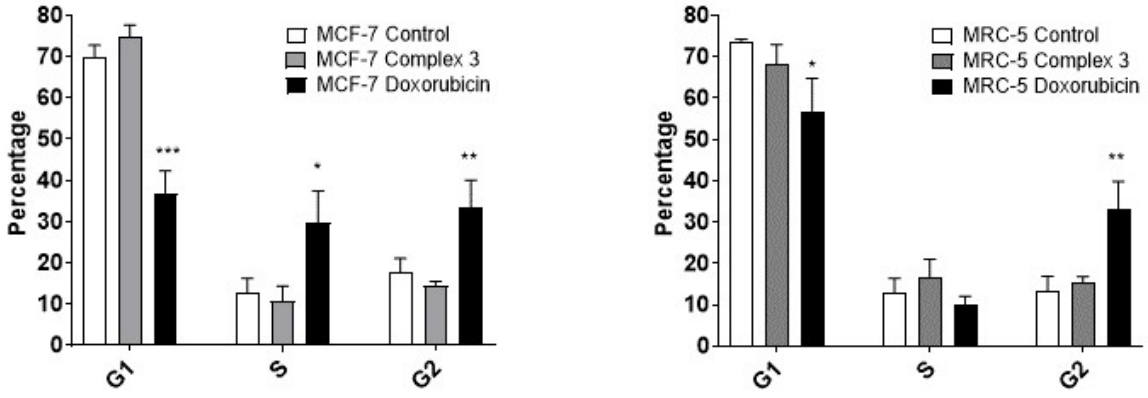

Figure S52. Cell cycle flow cytometry analysis of the MCF-7 breast adenocarcinoma cells and MRC-5 normal lung fibroblasts, showing the distribution of cells in the G1, S, and G2/M cell cycle phases after the treatment with complex **3** (10 μM) or doxorubicin (1 μM; positive control). The data points in the graph are the means ± SD of three independent experiments. Significance was tested using one-way ANOVA (*$p \leq 0.05$, **$p \leq 0.01$, *** $p \leq 0.001$).